DYNAMIC SNAP-THROUGH BUCKLING

OF ECCENTRICALLY STIFFENED SHALLOW SPHERICAL CAPS

A THESIS

Presented to

The Faculty of the Division of Graduate

Studies and Research

by

Charles McSween Blackmon

In Partial Fulfillment

of the Requirements for the Degree

Doctor of Philosophy

in the School of Aerospace Engineering

Georgia Institute of Technology

December, 1969

7/25/68

DYNAMIC SNAP-THROUGH BUCKLING

OF ECCENTRICALLY STIFFENED SHALLOW SPHERICAL CAPS

Approved:

Date approved by Chairman: _3/2/70_

ACKNOWLEDGMENTS

I would like to express my deepest appreciation to Dr. George J. Simitses for his suggestion of this problem and for his guidance throughout the course of this investigation. To Dr. Simitses and the members of my committee, Dr. C. V. Smith and Professor W. H. Horton, I owe special thanks for their careful reading of the manuscript.

The financial assistance of the National Aeronautics and Space Administration and the Georgia Institute of Technology are gratefully acknowledged.

Finally, I wish to thank my wife, Margaret, for her patience and help during the past three years.

TABLE OF CONTENTS

TABLE OF CONTENTS (Cont'd)

LIST OF TABLES

LIST OF ILLUSTRATIONS

LIST OF SYMBOLS

a_n	undetermined coefficients or generalized coordinates coordinates (nondimensional)
A_r, A_θ	cross-sectional area of the stiffeners, inch^2
D	flexural stiffness of the sheet, inch-pounds
D^s	smeared flexural stiffness of the stiffeners, inch-pounds
E	Young's modulus of elasticity, pounds/inch^2
E^p	extensional stiffness of the sheet, pounds/inch
E^s	extensional stiffness of the stiffeners, pounds/inch
e	stiffener eccentricity, inch
e_o	nondimensional rise of the sheet midsurface (H/h)
E_r, E_θ	Young's modulus for the stiffeners, pounds/inch^2
h	sheet thickness, inch
H	rise of the sheet midsurface, inch
I_r, I_θ	moment of inertia of the stiffener about its neutral axis, inch^4
I^*_{mp}	nondimensional impulse
I_{mp}	impulse per unit mass of the material, inches per second
ℓ_r, ℓ_θ	stiffener spacings, inch
$M_r, M_\theta, M_{r\theta}$	stiffened shell stress resultants per unit of midsurface length, pounds
$N_r, N_\theta, N_{r\theta}$	stiffened shell stress resultants per unit of midsurface length, pounds/inch
q	applied pressure, pounds/inch
Q	nondimensionalized applied pressure

List of Symbols (Cont'd.)

R radius of base of spherical cap, inch

R_o radius of spherical cap, inch

r, θ polar coordinates

t time, seconds

T^* nondimensionalized kinetic energy

T kinetic energy, pound-inch

T_i^* nondimensional initial kinetic energy imparted into the shell

T_d kinetic energy volume density, pounds/inch^2

T_i initial kinetic energy imparted into the shell, pound-inch

U_T^* nondimensional total potential energy

$\bar{U}$ strain energy density function, pounds/inch

U_T total potential energy, pound-inch

U_{T_d} total potential volume density, pounds/inch^2

u, v, w displacement components of the reference surface, inch

z distance to the undeformed reference surface from the r, θ-plane, inch

$\varepsilon_{rr}, \varepsilon_{\theta\theta}, \gamma_{r\theta}$ reference surface strains

η nondimensional normal displacement component (w/h)

$\kappa_{rr}, \kappa_{\theta\theta}, \kappa_{r\theta}$ changes in curvature and torsion at the reference surface, per inch

λ initial rise parameter $\left\{ 2[3(1-u^2)]^{1/4} (H/h)^{1/2} \right\}$

λ_o ratio of extensional stiffnesses of stiffener to sheet

μ Poisson's ratio

ξ dimensionless radial distance

List of Symbols (Cont'd.)

ρ ratio of the pressure at which the cap loses stability to the classical critical pressure for a complete sphere of thickness h

ρ_o ratio of flexural stiffnesses of stiffener to sheet

σ mass density of the material, pound-second^2 per inch^4

τ nondimensional time

ψ stress function in polar coordinates, pound-inch

∇^2 Laplacian operator in polar coordinates

∇^2_* nondimensional Laplacian operator

SUMMARY

The problem of snap-through buckling of a clamped, eccentrically stiffened shallow spherical cap is examined under quasi-static uniform pressure and two special cases of dynamic uniform pressure. These two dynamic cases considered are the impulsively applied (Dirac-delta function) loading and the instantaneously applied step (Heaviside function) loading with infinite duration. These are idealizations of the two extreme cases of blast loading, i.e., short decay times with large decay rates and large decay times with low decay rates respectively.

The analysis is based on nonlinear shallow shell equations (Marguerre) under the assumption of axisymmetric deformations and linear stress-strain laws. The eccentric stiffeners are placed orthogonally along lines of principal curvature in such a manner that the effective smeared thickness and the appropriate extensional and flexural stiffness are constant. The stiffeners are also taken to be one-sided with constant eccentricity, and the stiffener-shell combination is assumed monolithic.

A method is used in which critical pressures are associated with characteristics of the total potential surface in the configuration space of the generalized coordinates. The displacement is represented by a finite number of time-dependent coefficients (generalized coordinates) which are multiplied by the symmetric buckling modes of a clamped stiffened circular plate under uniform

radial compression applied around the circumference.

The results are presented in graphical form as load parameter versus initial rise parameter. Geometric configurations corresponding to isotropic, lightly stiffened, moderately stiffened and heavily stiffened geometries are considered. Lightly stiffened geometry implies that most of the extensional stiffness is provided by the thin skin. In a similar fashion, moderate stiffening implies the extensional stiffness of the skin and stiffeners are of the same magnitude and heavy stiffening implies that most of the extensional stiffness is provided by the stiffeners.

Two-term solutions appear to be good approximations for the range of values for which axisymmetric behavior prevails. This assertion is based on the fact that in the limiting condition when the stiffeners are reduced to zero the results agree with the known solutions for the isotropic shell.

By studying the generated data, the following important conclusions are drawn.

1) Eccentricity has a definite effect on the critical pressures of shallow caps.

2) Inside stiffeners yield a stronger configuration for both quasi-static and dynamic step loading conditions for which the two-term solution is valid.

3) For the same geometrical configuration, the critical pressure is lower for a dynamic load than for a quasi-static load.

4) For the ideal impulse, outside stiffeners yield the
   stronger configuration but the eccentricity effect is
   very small.

5) In all cases, buckling is possible for initial rise
   parameters higher than some minimum. The minimum value
   is approximately 3.2 for the isotropic configuration
   and increases as the value of eccentricity becomes larger.

CHAPTER I

INTRODUCTION

The need for structural efficiency in aircraft and missile structures is a well recognized fact. Thus structural instability, which can lead to failure, is a serious problem. Since thin-walled shallow spherical caps have many uses in modern aerospace structures, the question of how to make the most effective use of the material employed in their construction is important. Within the past several years studies have shown that eccentrically stiffened shells could be one answer to this problem. Typically, Harari, Singer and Baruch [1]* showed that by using eccentric stiffeners the buckling load to weight ratio of axially compressed circular cylinders could be increased by as much as fifty percent.

Structural elements are often subjected to both quasi-static and dynamic lateral loads which act toward the center of curvature. The typical response to such loading in shallow caps is snap-through buckling or oil canning and is characterized by a visible and sudden jump from one equilibrium configuration to another for which the displacements are larger than in the first. For the loading to be considered quasi-static, the time rate of load application must be of such magnitude that significant dynamic effects are not induced.

---

*Numbers in brackets following names refer to items in the References.

However, dynamic load application causes significant inertia effects which can substantially modify the critical conditions compared to the quasi-static case. Thus, a knowledge of the behavior in both circumstances is most desirable.

A large amount of experimental and analytical work has been done on the stability of monocoque cylindrical and spherical shells and on eccentrically stiffened cylindrical shells. Recently, Cole [2] performed a comprehensive parametric study of the effect of eccentric stiffeners on the buckling of complete spheres and indicated that considerable weight savings can be realized. His work also contains an excellent bibliography concerning eccentric stiffening effects on thin shells from the time the effects were first recognized by Van der Neut [3] to the present. There are, however, only a few studies, both analytical and experimental, of the buckling character-istics of spherical caps with non-uniform wall construction, and in these studies consideration was given only to quasi-static loading.

The study of the elastic stability of thin shallow isotropic spherical shells subjected to uniform pressure dates back to the investigations of von Kármán and Tsien [4]. Suhara [5] gives an historical summary of pertinent research prior to 1960. In more recent times, the critical impulse has been calculated by Humphreys and Bodner [6] using the Rayleigh-Ritz method. The same problem was also studied by Budiansky and Roth [7] using the Galerkin method. At the same time Budiansky and Roth solved the problem of dynamic snap-through under instantaneously applied uniform pressure with infinite

duration and reported results for a particular value of height-thickness ratio. Archer and Lange [8] treated this problem numerically by replacing the governing differential equations by finite difference equations.

Simitses [9] used a Ritz type procedure to find both the minimum possible dynamic load and impulse for snap-through for a wide range of the height to thickness parameter. Experimentally, Lock, Okubo and Whittier [10] measured the dynamic snap-through load for two values of the height-thickness ratio in which complete axisymmetric behavior was observed during snap-through. In recent works both Stephens and Fulton [11] and Stricklin and Martinez [12] determined critical snap-through loads which are in good agreement for a wide range of height-thickness ratios. These authors used finite difference and finite element displacement methods respectively. Huang [13], in a recent paper, integrated the non-linear differential equations by a finite difference method and an iterative procedure. He found critical loads for dynamic snap-through that are in good agreement with the results of the two last mentioned investigations [11-12].

The buckling of a clamped eccentrically stiffened spherical cap under quasi-static loading has been investigated by Bushnell [14-15] in recent papers using a finite difference technique. He, however, did not present an extensive parametric study of the stiffener eccentricity effect. Several other authors have made studies of the stability of eccentrically stiffened spherical domes under quasi-static

loading. Ebner [16] used an approximate method to calculate the general instability loads of meridionally stiffened shallow domes under uniform external pressure. In this work no account was taken of stiffener eccentricity. Crawford and Schwartz [17] calculated bifurcation loads from a membrane state for grid-stiffened spherical domes. They idealized the structure by considering it orthotropic and by neglecting the eccentricity of the stiffeners. In a later analysis, Crawford [18] derived constitutive relations in which the effect of eccentricity was included.

The problem, to be considered in this thesis, is the definition and analysis of axisymmetric snap-through buckling for an eccentrically stiffened clamped shallow spherical cap under quasi-statically applied uniform pressure and two special cases of dynamically applied uniform pressure. The latter two cases considered are the impulsively applied (Dirac-delta function) loading and the instantaneously applied step (Heaviside function) loading with infinite duration. In essence these are idealizations of blast loadings of short decay times with large decay rates and large decay times with low decay rates respectively. It is not the contention here that the blast loading problem is being solved but only the mathematical idealization of that problem.

CHAPTER II

GENERAL PROBLEM FORMULATION

The problem considered in this thesis is the definition and
analysis of axisymmetric snap-through buckling for eccentrically
stiffened clamped shallow spherical caps under quasi-statically applied
uniform pressure and two special cases of dynamically applied uniform
pressure. The latter two cases considered are the impulsively
applied (Dirac-delta function) loading and the instantaneously applied
(Heaviside function) loading with infinite duration.

The most direct way to approach the problem is to solve the
governing nonlinear differential equations for the dynamic and quasi-
static response of the structure subject to the appropriate initial and
boundary conditions. Bushnell [15] used a finite difference technique
and integrated these equations for a meridionally stiffened shallow
cap with a uniform pressure applied quasi-statically. In this manner
he found an approximate buckling load. Huang [13] investigated the
buckling characteristics of an isotropic shallow cap for quasi-static,
dynamic step and impulse loadings. He used finite difference equations
and an iterative scheme. A verification of the critical dynamic step
load for the isotropic shallow cap has been obtained by Stricklin and
Martinez [12] using a finite element displacement method.

Since the objective of this thesis is the determination of
critical loads and impulses, and not overall system response, the

problem was approached from a general energy viewpoint. The method
employed is similar to that used by Simitses [9] for the clamped
isotropic shallow shell and uses a Ritz type procedure. From the
quasi-static buckling problem of shallow caps Budiansky [19] noted
that the buckling load derived from an energy method deviates from
the exact solution somewhat. He emphasized that this deviation grows
with increases in the height-thickness ratio of the shell. It is
necessary, therefore, to examine the range of applicability of the
results obtained by this method.

General Method

All load cases considered do not explicitly depend on time and
exhibit such a load behavior that the total mechanical system is
conservative. Therefore Hamilton's integral, I, may be written as

$$I = \int_{t_1}^{t_2} \left[\int_{Vol} (T_d - U_{T_d}) \, dV \right] dt \tag{2.1}$$

where T_d is the kinetic energy volume density and U_{T_d} is the total
potential energy volume density. It should be noted that T_d and U_{T_d}
may be expressed solely in terms of the displacement components u, v
and w in the plane and normal to the plane of the circular boundary.

In the derivation of the kinetic and total potential energy
volume densities the following assumptions are made

    i) the deformation is axisymmetric,

    ii)   the effect of transverse shearing forces on the deformation

         is negligible,

   iii)   rotatory and in-plane kinetic energies are considered small

         compared to the normal kinetic energy.

The last assumption was justified by Reissner [20,21] for the isotropic

shell. It must be admitted that for the non-isotropic shell the

stiffeners do add to the rotatory and in-plane kinetic energies.

Nevertheless, since the analysis is generally limited by the require-

ments of thin shell theory, it is considered that these terms are

small relative to the normal kinetic energy and can be neglected.

     Applying Hamilton's principle, the extremization of Equation

(2.1) with respect to u and v yields the in-plane equation of motion

(in-plane equilibrium). These equations are not explicitly dependent

on time because of assumption iii). The third, or normal, equilibrium

equation is obtained by setting the generalized velocities equal to

zero and extremizing with respect to w. It should be noted that if

the character of motion of the cap midsurface was desired, the govern-

ing Euler-Lagrange differential equations of motion could be obtained

from extremizing with respect to w without setting the generalized

velocities equal to zero. These are not needed in the analysis,

however, since the critical loads and impulses are to be associated

with the total potential surface.

     A finite series of space-dependent functions with time-dependent

(in general) coefficients is assumed to represent the normal displace-

ment w with each term of the series satisfying the prescribed boundary

conditions. By assuming the deflection shape a priori, the internal

elastic strain energy may be associated with the shape amplitudes in

the following manner. A stress function which identically satisfies

in-plane equilibrium is used. This stress function is then related to

the normal displacement w through the compatibility equation and

associated boundary conditions. The use of this relation in the

expression for the total potential yields the total potential surface

in terms of the normal displacement w only. The time-dependent

coefficients are analogous to generalized coordinates, and the total

potential is thus a function of the loading, overall structural

geometry and the generalized coordinates, a_i.

Critical pressures for the case of quasi-static loading may be

found in the following manner. Setting the generalized velocities,

da_i/dt, equal to zero and applying the principle of the stationary

value of the total potential gives the static equilibrium points of a

conservative system. This implies

$$\frac{\partial U_T}{\partial a_i} = 0 \qquad i = 1, 2, \ldots \qquad (2.2)$$

at every static equilibrium point. Critical pressures for this case

are obtained by considering the stability in the small of these

equilibrium points through second variations. A snapping phenomenon

is possible if, and only if, the total potential surface in the space

of the generalized coordinates has at least three static equilibrium

points of which two are stable (one near and one far). The critical pressure is obtained when the near static equilibrium point ceases to be stable.

In considering the case of constant load with infinite duration, it is noted that for conservative and stationary systems the Hamiltonian is constant.

$$T + U_T = \text{constant} \tag{2.3}$$

The total potential can be defined such that, if the initial kinetic energy is zero, the constant will be zero.

$$T + U_T = 0 \tag{2.4}$$

If the kinetic energy is a positive definite quantity, the presence of buckled or unbuckled motion* can be determined by examining the total potential surface. (For the present solution it can be shown that the kinetic energy is indeed a positive definite function of the generalized velocities.) Since the minimum possible critical load will occur when the shell snaps through with zero velocity, the kinetic energy will be zero and thus at snap-through

$$U_T = 0 \tag{2.5}$$

---

*See page 13 for a definition of buckled and unbuckled motion.

at the unstable static equilibrium point. Also there must exist a possible motion from the undeformed shape to the unstable equilibrium configuration.

For the case of the ideal impulsive load, the critical impulses can also be associated with characteristics of the total potential surface. Every particle of the system is assumed to be instantaneously accelerated to a known finite velocity before any displacement occurs, and for all times $t > 0$ there is no further external load applied. The work done by the ideal impulsive load is imparted into the system instantaneously as initial kinetic energy. A critical impulse is that impulse which imparts such kinetic energy to the system that the resulting motion is a buckled one. The equation of energy may be written as

$$T + U_T = T_{initial}. \tag{2.6}$$

In order for this type of buckling to occur the initial rise magnitude must be such that the zero load potential surface has at least three stationary values. The impulse is considered critical if the zero-load unstable static equilibrium position is reached with zero kinetic energy. Thus through the equation

$$U_{T_{impulse}} = T_{initial} \tag{2.7}$$

the critical impulse may be related to the total potential.

Demonstration of the Method for One Degree of Freedom

Assuming that the deformation is represented by a single mode, the total potential surface will then be a function of a single generalized coordinate, the magnitude of the applied load and the structural configuration. Consider the family of curves which are shown in Figure 1. Each curve represents a different level of applied loading. However, all represent a particular cap with no change in structural configuration between load levels. The points A_i, B_i and C_i denote the static equilibrium points for each loading, q_i.

The instantaneous application of constant magnitude, infinite duration load q_1 results in an unbuckled motion, and the system oscillates non-linearly about the near static equilibrium position A_1. If the load q_2 is applied suddenly, it is now possible for the system to reach the unstable equilibrium position B_2 with zero velocity (kinetic energy) and possibly snap through towards the far stable equilibrium position C_2. At load levels, q_3, q_4, the system will definitely snap through and perform nonlinear oscillations about points C_3, C_4. It is seen from this single degree of freedom example that at q_1 the motion is unbuckled, while at q_2 buckling is possible, and the corresponding load is thus the minimum possible critical load for constant magnitude, infinite duration. It is noted that q_4 represents the critical load for the quasi-static case since the near static equilibrium point ceases to be stable.

The curve representing the zero load level q_o furnishes the information needed to find the critical impulse for the ideal impulse
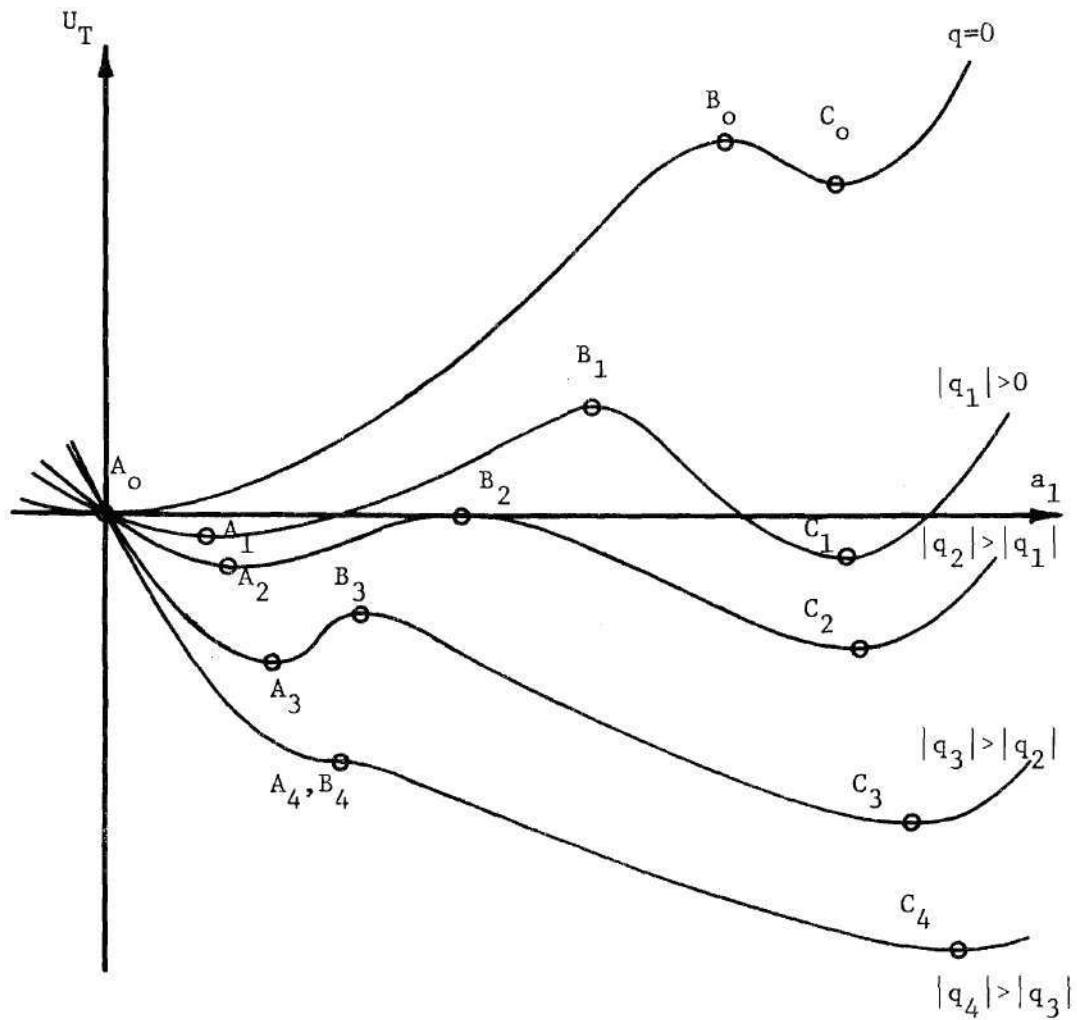
Figure 1. Total Potential Curve in the Configuration Space of the Generalized Coordinate a_1.

loading case. Assuming that the rise is of such magnitude that the potential surface has at least three stationary points, then the potential energy at the unstable equilibrium point B_o can be related to the critical impulse through the initial kinetic energy imparted into the system necessary to reach B_o.

The explanation thus cited can be extended to a deformation pattern dependent on two or more modes. In the case of two modes the potential can be represented as a series of surfaces in two generalized coordinates and can be easily examined. For three or more modes, however, each loading condition is represented by a hypersurface which in most cases is not easily visualized. In cases of two or more modes, the unstable equilibrium points need not be relative maxima of the surface but may be saddle points.

On the basis of the foregoing explanation the following definitions as given by Simitses [9] have been used.

possible locus: A possible locus on the surface is one which corresponds at every point of the locus to a non-negative kinetic energy.

unbuckled motion: Unbuckled motion of the system is defined as any possible locus on the total potential surface which completely encloses only the near equilibrium point.

buckled motion: If the possible locus passes through or encloses other equilibrium points, or, if the near equilibrium point becomes unstable, the motion is defined as buckled, and the system has "snapped through".

<u>Minimum Possible Critical Dynamic Conditions</u>

As pointed out by Humphreys [22], the critical impulse and critical dynamic load obtained by the energy method may not be correct. However, it will now be shown that the result obtained by this method will always be a lower bound for the critical load or impulse.

First consider the case of impulsive loading. The total potential energy surface is given by the surface associated with zero external load. When $U_{T_{imp}}$ is the smallest magnitude of potential energy corresponding to a point of unstable equilibrium and in addition, there exists a path from the undeformed configuration to that unstable point along which path $U_{T_d} < U_{T_{imp}}$, then this point will be called the first unstable equilibrium point. It should be noted that when the external load is zero $U_{T_d} = U$, the strain energy. The strain energy is, of course, positive except for the undeformed state, in which case it has zero value. If T_i denotes the initial kinetic energy imparted to the system by the impulse, then during subsequent motion of the system in the configuration space

$$T + U_{T_d} = T_i \qquad (2.8)$$

or

$$T = T_i - U_{T_d} \quad . \qquad (2.9)$$

Clearly, if $T_i < U_{T_{imp}}$, the system can never reach the first unstable equilibrium configuration since negative kinetic energy would be necessary. If, however,

$$T_i = U_{T_{imp}} \qquad\qquad (2.10)$$

then there is a possibility of snap-through buckling and $U_{T_{imp}}$ represents a lower bound on the required initial kinetic energy.

Next, consider the case of suddenly applied load. As the load increases in magnitude, the level of the total potential corresponding to the unstable static equilibrium points decreases. Let q_D represent the magnitude of external load for which the value of the total potential at one static equilibrium point is zero and a possible locus to that unstable point exists. Now, if $q < q_D$, there are two possibilities, either

    i)   all unstable equilibrium points have positive total
         potential energy, in which case there is no possible locus
         to those points, or

   ii)   some unstable static equilibrium points might correspond to
         a nonpositive potential but no possible locus.

In no circumstance is there a way for the system to reach an unstable static equilibrium point if $q < q_D$. Therefore, q_D represents a lower bound on external loads for snap-through.

The differential equations of motion are not solved when the energy method is used and thus the actual trajectory of the system on

the total potential energy surface is not known. This means that if $q = q_D$ the path of the system given by the solution to the differential equations might not include an unstable equilibrium point. The true critical load might, therefore, be greater than q_D, but it certainly cannot be less. It must be emphasized that U_{T_d} and q_D represent lower bounds for buckled motion.

One other point should be noted. The energy method provides true lower bounds only for the mechanical system whose energy is actually formulated. Thus, if a continuous system is approximated by an "n" degree of freedom discrete system, and the energy is then formulated for that discrete system, the resulting lower bounds are true only for the discrete system. The extent of applicability of the discrete system bounds to the continuous system depends on the accuracy of the approximation.

In this thesis, the applicability of the results has been judged by comparisons with data derived from the "exact" solution for the isotropic shell.

CHAPTER III

GOVERNING EQUATIONS FOR THE STIFFENED CAP

A thin shallow spherical cap is stiffened eccentrically in
the circumferential and meridional directions as shown in Figure 2
such that

  i) the stiffeners are both on the same side,

  ii) the stiffener eccentricity is the same for all stiffeners
      and is constant,

  iii) the smeared extensional and flexural stiffnesses are the
       same along both the circumferential and meridional
   directions and are constant.

Governing Equations

The basic geometry and notation for a clamped shallow spherical
cap are shown in Figures 3 and 4. The nonlinear strain-displacement
and curvature-displacement relations known as the shallow shell or
Marguerre equations as reported by Sanders [23] are used. These
equations are based on

  i) small strains,

  ii) moderately small rotations with rotations about the normal
      being neglected,

  iii) the Donnell-Mushtari-Vlasov approximation.

In addition it is assumed that the shell deforms in an axisymmetric
mode. Under these assumptions the following basic relations can be
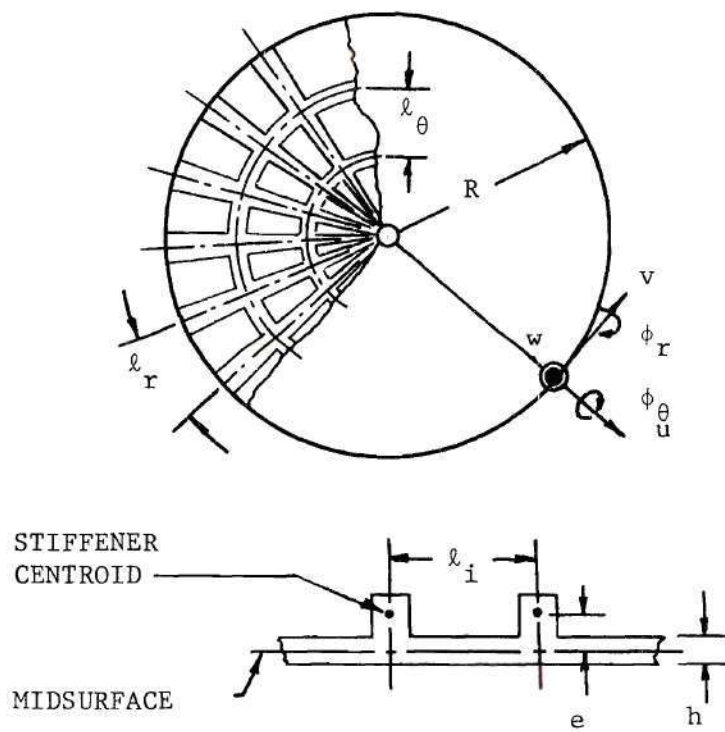
Figure 2. Geometry of Stiffener Placement.
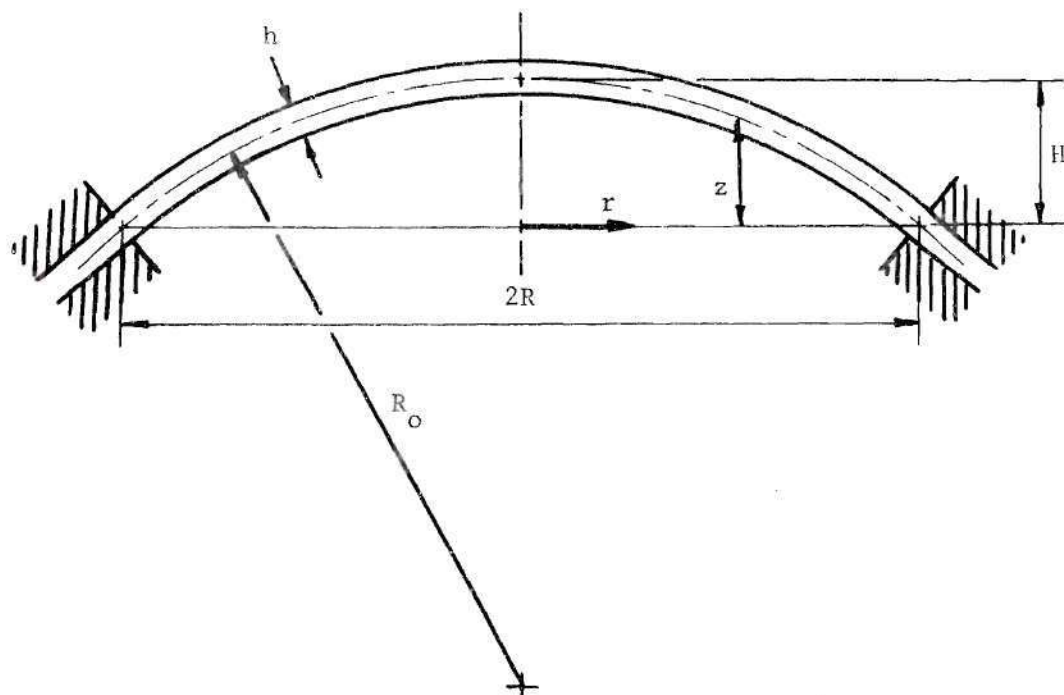
Figure 3. Geometry of Clamped Shallow Spherical Shells.
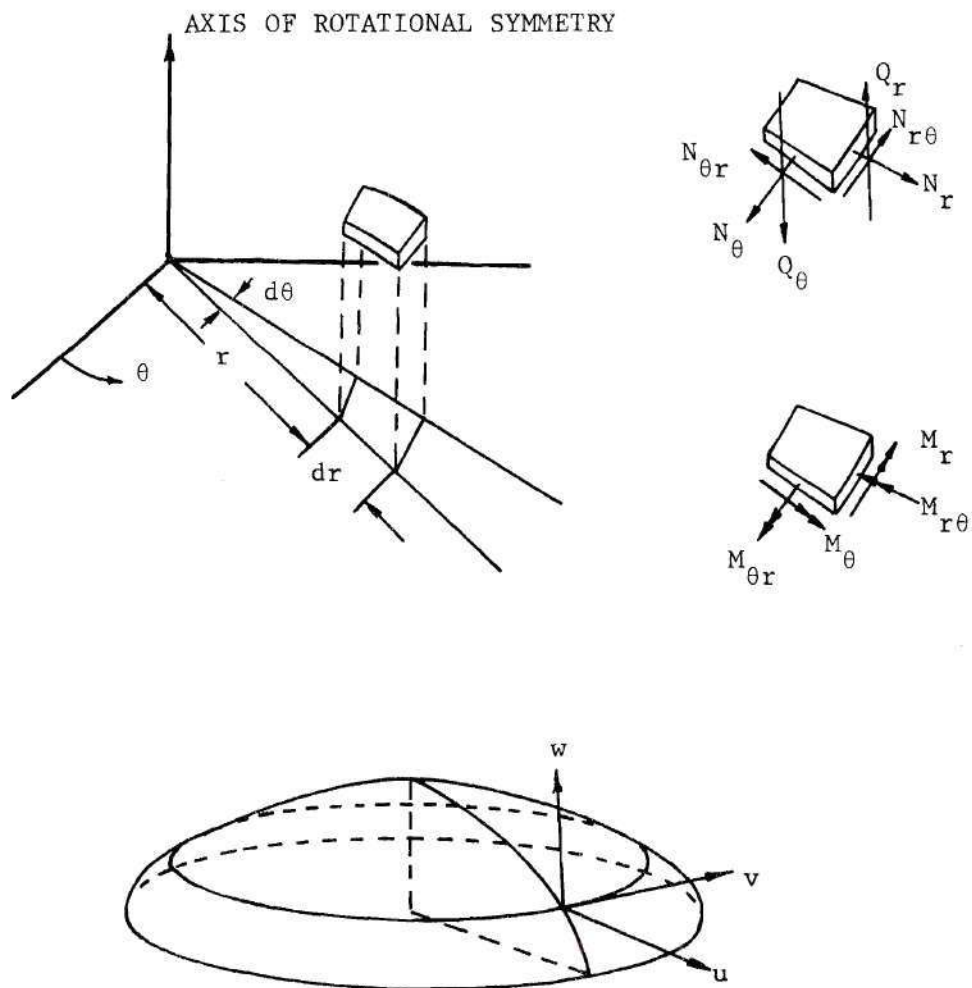
Figure 4. Notation and Sign Convention

written using the midsurface of the skin as the reference.

$$\varepsilon_{rr} = u,_r + z,_r w,_r + \frac{1}{2} (w,_r)^2$$

$$\varepsilon_{\theta\theta} = \frac{u}{r} \qquad\qquad (3.1)$$

$$\gamma_{r\theta} = 0$$

$$\kappa_{rr} = -w,_{rr}$$

$$\kappa_{\theta\theta} = -\frac{1}{r} w,_r \qquad\qquad (3.2)$$

$$\kappa_{r\theta} = 0$$

In the derivation of the constitutive relations for the combined sheet-stiffener system, as shown in Figure 2, the Kirchhoff-Love hypotheses as modified by Baruch and Singer [24] are used. The stiffeners follow lines of principal curvature and are close enough to be smeared. The eccentricity effect, or height of the stiffener center of gravity above the midsurface is retained by assuming that the strain varies linearly through the actual thickness of the stiffeners and not through a smeared-out or "effective" thickness. The strains at any material point may be expressed in terms of the reference surface strains and changes in curvature and torsion.

$$\varepsilon_r = \varepsilon_{rr} + z\kappa_{rr}$$

$$\varepsilon_\theta = \varepsilon_{\theta\theta} + z\kappa_{\theta\theta} \qquad\qquad (3.3)$$

$$\gamma = \gamma_{r\theta} + 2z\kappa_{r\theta}$$

Assuming that before, and at the instant of buckling, no material point is stressed beyond the proportional limit and that the Poisson effect on the stiffener is negligible the following stress-strain relations may be written:

for the skin

$$\sigma_r^p = \frac{E}{1 - \mu^2} (\varepsilon_r + \mu\varepsilon_\theta) \ ;$$

$$\sigma_\theta^p = \frac{E}{1 - \mu^2} (\varepsilon_\theta + \mu\varepsilon_r) \ ; \qquad\qquad (3.4)$$

$$\tau_{r\theta} = \frac{E}{2(1 + \mu)} \gamma$$

and for the stiffeners

$$\sigma_r^s = E_r \varepsilon_r \ ;$$

$$\sigma_\theta^s = E_\theta \varepsilon_\theta \ . \qquad\qquad (3.5)$$

It is assumed that the shear is carried entirely by the sheet.

Denoting by N_r, N_θ and $N_{r\theta}$ the stress resultants and M_r, M_θ and $M_{r\theta}$ the moment resultants of the combined system the following may be written:

$$\left.\begin{array}{l} N_i = \displaystyle\int_{-h/2}^{h/2} \sigma_i^P dz + \frac{1}{\ell_i} \int_{A_i} \sigma_i^s \, d\,A_i \; ; \\[2em] M_i = \displaystyle\int_{-h/2}^{h/2} \sigma_i^P z dz + \frac{1}{\ell_i} \int_{A_i} \sigma_i^s \, z \, d\,A_i \,. \end{array}\right\} \quad (3.6)$$

Performing the indicated operations the constitutive relations for the eccentrically stiffened shell become

$$\left.\begin{array}{l} N_r = (E^P + E_r^s)\epsilon_{rr} + \mu E^P \epsilon_{\theta\theta} + e_r E_r^s \kappa_{rr} \\[1.5em] N_\theta = \mu E^P \epsilon_{rr} + (E^P + E_\theta^s)\epsilon_{\theta\theta} + e_\theta E_\theta^s \kappa_{\theta\theta} \\[1.5em] N_{r\theta} = \dfrac{Eh}{2(1+\mu)} \; \gamma_{r\theta} \end{array}\right\} \quad (3.7)$$

$$\left.\begin{array}{l} M_r = (D + D_r^s)\kappa_{rr} + \mu D \kappa_{\theta\theta} + e_r^2 E_r^s \kappa_{rr} + e_r E_r^s \epsilon_{rr} \\[1.5em] M_\theta = \mu D \kappa_{rr} + (D + D_\theta^s)\kappa_{\theta\theta} + e_\theta^2 E_\theta^s \kappa_{\theta\theta} + e_\theta E_\theta^s \epsilon_{\theta\theta} \end{array}\right\} \quad \begin{array}{l}(3.8\\ \text{Cont.)}\end{array}$$

$$M_{r\theta} = D(1 - \mu)\kappa_{r\theta} \qquad (3.8)$$

where

$$E^P = \frac{Eh}{1 - \mu^2} \; ; \qquad E^S_r = \frac{E_r A_r}{\ell_r} \; ; \qquad E^S_\theta = \frac{E_\theta A_\theta}{\ell_\theta} \; ;$$

$$D^S_\theta = \frac{E_\theta I_{\theta_{c.g.}}}{\ell_\theta} \; ; \qquad D^S_r = \frac{E_r I_{r_{c.g.}}}{\ell_r} \; ; \qquad D = \frac{Eh^3}{12(1 - \mu^2)} \; . \qquad (3.9)$$

A_i and $I_{i_{c.g.}}$ are respectively the cross-sectional area and the second moment of the area about centroidal axes of the stiffeners.

Next, if A_r and $I_{r_{c.g.}}$ are taken to vary linearly in the plane of u and v, as ℓ_r does, then E^S_r and D^S_r are constant. It should be noted that although ℓ_r is the measured distance between the centroids of adjacent radial stiffeners and is not linear, it is assumed linear since the shell under consideration is shallow. Furthermore, letting $E^S_r = E^S_\theta = E^S$, $D^S_r = D^S_\theta = D^S$ and $e_r = e_\theta = e$ and making the axisymmetric deformation assumption the constitutive relations become

$$N_r = (E^P + E^S)\varepsilon_{rr} + \mu E^P \varepsilon_{\theta\theta} + e E^S \kappa_{rr} \; ;$$

$$N_\theta = \mu E^P \varepsilon_{rr} + (E^P + E^S)\varepsilon_{\theta\theta} + e E^S \kappa_{\theta\theta} \; ; \qquad (3.10)$$

$$N_{r\theta} = 0 \; ;$$

$$M_r = (D + D^S)\kappa_{rr} + \mu D\kappa_{\theta\theta} + e^2 E^S \kappa_{rr} + eE^S \varepsilon_{rr} \; ;$$

$$M_\theta = \mu D\kappa_{rr} + (D + D^S)\kappa_{\theta\theta} + e^2 E^S \kappa_{\theta\theta} + eE^S \varepsilon_{\theta\theta} \; ; \qquad \Biggr\} \qquad (3.11)$$

$$M_{r\theta} = 0 \; .$$

On the basis of the assumptions made, the following expressions may be written for the energies

$$T = \pi\sigma h \int_o^R w_{,t}^2 \; rdr \; ; \qquad (3.12)$$

$$U_T = 2\pi \int_o^R (\bar{U} - qw)rdr \qquad (3.13)$$

where $\bar{U}$ is the strain energy density function

$$\bar{U} = \frac{1}{2} (N_r\varepsilon_{rr} + N_\theta\varepsilon_{\theta\theta} + M_r\kappa_{rr} + M_\theta\kappa_{\theta\theta}) \qquad (3.14)$$

and q is the applied uniform pressure positive in the positive w direction.

The total potential, U_T, can be written entirely in terms of the displacements u, v and w and their spatial derivatives by using the strain-displacement, curvature-displacement and constitutive relations.

$$U_T = 2\pi \int_{0}^{R} \left[\!\!\left[-qw + \frac{1}{2}\left\{ (E^P + E^S)\left[(u,_r + z,_r w,_r + \frac{1}{2} w,_r^2)^2 + (\frac{u}{r})^2 \right] \right.\right.$$

$$+ 2\mu E^P (u,_r + z,_r w,_r + \frac{1}{2} w,_r^2)(\frac{u}{r}) + (D + D^S + E^S e^2)(w,_{rr}^2 + \frac{1}{r^2} w,_r^2)$$

$$\text{(3.15)}$$

$$+ 2\mu D \frac{w,_r}{r} w,_{rr} - 2 E^S e[(u,_r + z,_r w,_r + \frac{1}{2} w,_r^2)w,_{rr}$$

$$+ \frac{u}{r^2} w,_r]\left.\left.\right\}\right]\!\!\right] rdr$$

Although the equilibrium equations are not needed in this method of analysis, they are derived through the principle of the stationary value of the total potential and are presented herein for sake of completeness. Because of axisymmetric behavior the equations of equilibrium are

$$N_\theta - (rN_r),_r = 0; \qquad \text{(3.16)}$$

$$qr + (rM_r),_{rr} + N_\theta (z + w),_r + rN_r(z + w),_{rr} - M_{\theta,r} = 0. \quad \text{(3.17)}$$

The compatibility equation for the cap can be written in the following manner by using the strain-displacement relations and assuming that the initial midsurface shape is characterized by $z = z(r)$.

$$\varepsilon_{\theta\theta,rr} + \frac{2}{r}\varepsilon_{\theta\theta,r} - \frac{1}{r}\varepsilon_{rr,r} = -z_{,rr}\frac{w_{,r}}{r} - w_{,rr}\frac{w_{,r}}{r} - \frac{1}{r}z_{,r}w_{,rr} \qquad (3.18)$$

The in-plane equation of equilibrium can be identically satisfied by introducing a stress function defined as follows:

$$\left.\begin{aligned} N_r &= \frac{1}{r}\psi_{,r} \\[2em] N_\theta &= \psi_{,rr} \end{aligned}\right\} \qquad (3.19)$$

By using this stress function and other substitutions, the equilibrium and compatibility equations can be written solely in terms of w and ψ. In this manner the equilibrium equation becomes

$$\left[1 + \rho_o + 12\lambda_o\frac{e^2}{h^2}\right]\nabla^4 w - 12\,\lambda_o^2\frac{e^2}{h^2}\frac{1+\lambda_o}{[(1+\lambda_o)^2 - \mu^2]}\nabla^4 w$$

$$= \frac{q}{D} - \frac{e\lambda_o\mu}{D[(1+\lambda_o)^2 - \mu^2]}\nabla^4\psi + \frac{\psi_{,rr}}{D}\left(\frac{z_{,r} + w_{,r}}{r}\right) \qquad (3.20)$$

$$+ \frac{\psi_{,r}}{D}\left(\frac{z_{,rr} + w_{,rr}}{r}\right)$$

and the compatibility equation is

$$(1 + \lambda_o) \, \nabla^4 \psi = e \lambda_o \mu \, E^P \nabla^4 w - E^P \left[(1 + \lambda_o)^2 - \mu^2 \right] \left[\frac{1}{r} w,_r (z,_{rr} + w,_{rr}) \right.$$

$$\left. + \frac{1}{r} w,_r z,_r \right] \tag{3.21}$$

where for rotationally symmetric deformations

$$\nabla^4 = \frac{d^4}{dr^4} + \frac{2}{r} \frac{d^3}{dr^3} - \frac{1}{r^2} \frac{d^2}{dr^2} + \frac{1}{r^3} \frac{d}{dr} \tag{3.22}$$

and the constants λ_o and ρ_o are defined by

$$\lambda_o = \frac{E^S}{E^P} \quad ; \qquad \rho_o = \frac{D^S}{D} \quad . \tag{3.23}$$

Boundary Conditions

The edge of the shell is completely clamped; therefore on the boundary $r = R$

$$w = 0; \quad w,_r = 0; \quad u = 0; \quad v = 0. \tag{3.24}$$

The condition $v = 0$ is identically satisfied since axisymmetric

deformations are assumed. From the condition u = 0 it follows that

$$\varepsilon_{\theta\theta} = 0 \qquad (3.25)$$

on the boundary r = R.

By the substitution of the constitutive relations and the stress function into the boundary condition $\varepsilon_{\theta\theta} = 0$ the following important relation is obtained at r = R.

$$\psi,_{rr} - \frac{\mu}{1 + \lambda_o} \frac{\psi,_r}{R} = -eE^s \left[\frac{w,_r}{R} - \frac{\mu}{1 + \lambda_o} w,_{rr} \right] \qquad (3.26)$$

Using the condition that $w,_r = 0$ at the boundary in Equation (3.26), the complete set of boundary conditions becomes

$$w = 0 \; ; \qquad (3.27)$$

$$w,_r = 0 \; ; \qquad (3.28)$$

$$\psi,_{rr} - \frac{\mu}{1 + \lambda_o} \frac{\psi,_r}{R} = \frac{eE^s \mu}{1 + \lambda_o} w,_{rr} \; . \qquad (3.29)$$

In addition, the auxiliary condition that all stresses and displacements at the center (r = 0) of the shell must remain finite is also imposed on the problem.

Total Potential

Although the total potential has been previously derived
(Equation (3.15)) in terms of the displacements u, v and w, it is
necessary in this analysis to have this equation expressed entirely
in terms of the normal displacement, w. This is done by various
substitutions which are omitted for the sake of brevity. These
substitutions give the total potential in terms of the stress function
ψ and w. Then, solving the compatibility equation for ψ with the
proper boundary conditions for the clamped shallow shell and substitu-
ting for ψ yields the total potential equation as a function of w only.
The details of this procedure are presented in Appendices A and B.
The total potential for the clamped shell can be written as

$$U_T = \frac{\pi}{\beta_o} \int_o^R \left\{ \alpha_o^2 \left(w,_{rr} + \frac{w,_r}{r} \right)^2 + \frac{\beta_o^2}{4} \left(\int_o^r \frac{w,_x^2}{x} dx \right)^2 + \left(\frac{2H\beta_o w}{R^2} \right)^2 + c_o^2 \right.$$

$$+ \left(w,_{rr} + \frac{w,_r}{r} \right) \left[2\alpha_o C_o + \frac{4H}{R^2} \alpha_o \beta_o w - \alpha_o \beta_o \int_o^r \frac{w,_x^2}{x} dx \right]$$

$$\left. - \left[\frac{2H}{R^2} \beta_o^2 w + C_o \beta_o \right] \int_o^r \frac{w,_x^2}{x} dx + \frac{4H}{R^2} \beta_o C_o w \right\} r dr \qquad \begin{array}{c} (3.30 \\ \text{Cont.)} \end{array}$$

$$- \frac{\pi}{\beta_o} \left(\frac{1 + \lambda_o + \mu}{1 + \lambda_o} \right) \left\{ - \frac{\beta_o}{2R} \int_o^R r \left(\int_o^r \frac{w,_x^2}{x} dx \right) dr + \frac{2 H\beta_o}{R^3} \int_o^R wr\, dr \right.$$

$$+ \left. \frac{C_o R}{2} \right\}^2 - \pi \left\{ \frac{(e E^s)^2}{\beta_o} - D \left(1 + \rho_o + 12 \lambda_o \frac{e^2}{h^2} \right) \right\} \int_o^R \left(w,_r + \frac{w,_r}{r} \right)^2 r dr$$

$$- 2 \pi \int_o^R qwrdr$$

where

$$\alpha_o = e \left(\frac{\lambda_o}{1 + \lambda_o} \right) \mu E^p \quad ; \tag{3.31}$$

$$\beta_o = \frac{E^p}{1 + \lambda_o} [(1 + \lambda_o)^2 - \mu^2] \tag{3.32}$$

and

$$C_o = \beta_o \left(\frac{1 + \lambda_o + \mu}{1 + \lambda_o - \mu} \right) \left\{ \frac{1 + \lambda_o}{1 + \lambda_o + \mu} \int_o^R \frac{w,_r^2}{r} dr - \frac{1}{R^2} \int_o^R r \left(\int_o^r \frac{w,_x^2}{x} dx \right) dr \right.$$

$$\tag{3.33}$$

$$\left. + \frac{4H}{R^4} \int_o^R rwdr \right\} .$$

Nondimensionalization

It is convenient to express all quantities involved in nondimensional form. Consistent with this the following relations are used:

$$\xi = \frac{r}{R} \; ; \qquad \eta = \frac{w}{h} \; ; \qquad e_o = \frac{H}{h} \; ; \qquad \eta_o = \frac{z}{h} \; ;$$

$$(\;)' = \frac{d}{d\xi} \; ; \qquad \nabla_*^2 = \frac{d^2}{d\xi^2} + \frac{1}{\xi} \frac{d}{d\xi} \quad ;$$

$$Q(\xi,\tau) = \frac{(1 - \mu^2)R^4}{Eh^4} \; q(r,t) \; .$$

Using the quantities defined above the following nondimensional expression related to the total potential is obtained:

$$U_T^* \; = \; \frac{(1 - \mu^2)R^2}{2 \, \pi Eh^5} \; U_T \; .$$

The following nondimensional constants

$$B_1 = \frac{e\lambda_o \mu}{h(1 + \lambda_o)} \; ; \tag{3.34}$$

$$B_2 = \frac{(1 + \lambda_o)^2 - \mu^2}{1 + \lambda_o} \; ; \tag{3.35}$$

$$B_3 = \frac{1 + \lambda_o + \mu}{1 + \lambda_o - \mu} \tag{3.36}$$

and the expression

$$B_o = \frac{1 + \lambda_o}{1 + \lambda_o + \mu} \int_o^1 \frac{n^2_{,\xi}}{\xi} d\xi - \int_o^1 \xi \left(\int_o^\xi \frac{n^2_{,x}}{x} dx \right) d\xi + 4e_o \int_o^1 \xi n d\xi \qquad (3.37)$$

are used to derive a nondimensional expression for the total potential. This can be written as

$$U_T^* = \frac{1}{2} \frac{B_1^2}{B_2} \int_o^1 (\nabla_*^2 n)^2 \xi d\xi + \frac{B_2}{8} \int_o^1 \left(\int_o^\xi \frac{n^2_{,x}}{x} dx \right)^2 \xi d\xi + 2e_o^2 B_2 \int_o^1 n^2 \xi d\xi$$

$$+ \frac{1}{4} B_2 B_3^2 B_o^2 + B_1 B_3 B_o \int_o^1 \nabla_*^2 n \; \xi d\xi + 2e_o B_1 \int_o^1 n \nabla_*^2 n \; \xi d\xi$$

$$- \frac{B_1}{2} \int_o^1 \nabla_*^2 n \left(\int_o^\xi \frac{n^2_{,x}}{x} dx \right) \xi d\xi - e_o B_2 \int_o^1 n \left(\int_o^\xi \frac{n^2_{,x}}{x} dx \right) \xi d\xi \qquad \begin{array}{l}(3.38 \\ \text{Cont.})\end{array}$$

$$- \frac{1}{2} B_2 B_3 B_o \int_o^1 \left(\int_o^\xi \frac{n^2_{,x}}{x} dx \right) \xi d\xi + 2e_o B_2 B_3 B_o \int_o^1 n \xi d\xi$$

$$- \frac{1}{2} (1 + \lambda_o + \mu)[(1 + \lambda_o)^2 - \mu^2] \left[\frac{B_o}{1 + \lambda_o - \mu} \right.$$

$$- \frac{1}{2(1 + \lambda_o + \mu)} \left[\int_0^1 \frac{\eta,_\xi^2}{\xi} d\xi \right]^2 - \frac{1}{24} \left\{ 12 \frac{B_1^2}{B_2} \left(\frac{1 + \lambda_o}{\mu} \right)^2 \right.$$

$$\left. - \left(1 + \rho_o + 12 \lambda_o \frac{e^2}{h^2} \right) \right\} \int_0^1 (\nabla_*^2 \eta)^2 \xi d\xi - Q \int_0^1 \eta \xi d\xi .$$

General Solution Procedures

Although the initial shape of the midsurface is assumed to be spherical, the meridional curve is approximated by the parabola

$$\eta_o(\xi) = e_o(1 - \xi^2) . \tag{3.39}$$

The shallow cap is clamped along its circular boundary. Thus the boundary conditions associated with the normal displacement, w, are expressed in nondimensional form as

$$\eta(1,\tau) = 0 ; \tag{3.40}$$

$$\eta'(1,\tau) = 0 ; \tag{3.41}$$

where

$$(\ )' = \frac{d}{d\xi} .$$

The nondimensional vertical displacement parameter, η, is expressed by the following series

$$\eta = \sum_{n=1}^{\infty} a_n(\tau) [J_o(k_n^1 \xi) - J_o(k_n^1)] \qquad (3.42)$$

where k_n^1 are the zeroes of $J_1(x) = 0$ and each term of the series satisfies the boundary conditions. The functions $[J_o(k_n^1 \xi) - J_o(k_n^1)]$ represent the axisymmetric buckling modes of an eccentrically stiffened flat circular plate loaded by a uniformly applied edge thrust. These expressions are derived in Appendix C. For the dynamic cases considered the time-dependent coefficients, $a_n(\tau)$, are thought of as generalized coordinates and the time history of the displacement is defined in terms of these coordinates. For the quasi-static case, however, these coefficients become undetermined constants.

It is convenient now to define certain integrals which occur in the expression for the total potential energy, Equation (3.38). The following relations for the integrals are obtained by employing well-known properties of Bessel functions (the superscript "1" on k_n is dropped for convenience):

$$\int_o^1 (\nabla_*^2 \eta)^2 \xi d\xi = \frac{1}{2} \sum_{n=1}^{\infty} a_n^2 k_n^4 J_o^2(k_n) \qquad (3.43)$$

and

$$\int_0^\xi \frac{n_{,x}^2}{x} \, dx = \sum_{n=1}^\infty \sum_{m=1}^\infty a_n a_m \phi_{nm}(\xi) \tag{3.44}$$

where

$$\phi_{nm}(\xi) = \int_0^\xi \frac{k_n k_m}{x} J_1(k_m x) J_1(k_n x) dx \; . \tag{3.45}$$

Also by defining

$$\gamma_{nmpq} = \int_0^1 \phi_{nm}(\xi) \phi_{pq}(\xi) \xi d\xi \tag{3.46}$$

the following expression is obtained

$$\int_0^1 \xi \left(\int_0^\xi \frac{n_{,x}^2}{x} \, dx \right)^2 d\xi = \sum_{n=1}^\infty \sum_{m=1}^\infty \sum_{p=1}^\infty \sum_{q=1}^\infty a_n a_m a_p a_q \gamma_{nmpq} \tag{3.47}$$

and it can be shown that

$$\int_0^1 n^2 \xi d\xi = \frac{1}{2} \sum_{n=1}^\infty a_n^2 J_o^2(k_n) + \frac{1}{2} \sum_{n=1}^\infty \sum_{m=1}^\infty a_n a_m J_o(k_n) J_o(k_m) \; ; \tag{3.48}$$

$$\int_0^1 \nabla_*^2 n \xi d\xi = 0 \; ; \tag{3.49}$$

$$\int_1^o n \nabla_*^2 n\,\xi d\xi = -\frac{1}{2} \sum_{n=1}^\infty a_n^2 k_n^2 J_o^2(k_n) \quad ; \tag{3.50}$$

$$\int_1^o n\,\xi d\xi = -\frac{1}{2} \sum_{n=1}^\infty a_n J_o(k_n) \quad ; \tag{3.51}$$

$$\int_1^o \xi \left(\int_{n,x}^o \frac{\xi^2}{x}\,dx \right) d\xi = \sum_{n=1}^\infty \sum_{m=1}^\infty a_n a_m \alpha_{nm} \quad ; \tag{3.52}$$

$$\int_1^o n \left(\int_{n,x}^o \frac{\xi^2}{x}\,dx \right) \xi d\xi = \sum_{n=1}^\infty \sum_{m=1}^\infty \sum_{p=1}^\infty a_n a_m a_p [\tau_{nmp} - J_o(k_n)\alpha_{mp}] \quad ; \tag{3.53}$$

$$\int_1^o \nabla_*^2 n \left(\int_{n,x}^o \frac{\xi^2}{x}\,dx \right) \xi d\xi = - \sum_{n=1}^\infty \sum_{m=1}^\infty \sum_{p=1}^\infty a_n a_m a_p k_n^2 \tau_{nmp} \tag{3.54}$$

where

$$\alpha_{nm} = \int_1^o \xi\, \phi_{nm}(\xi)\, d\xi \quad ; \tag{3.55}$$

$$\tau_{nmp} = \int_1^o J_o(k_n\xi)\phi_{mp}(\xi)\xi d\xi \quad . \tag{3.56}$$

By using the integrals defined above the nondimensional expression for the total potential is a polynomial of fourth order in the generalized coordinates.

$$U_T^* = \frac{1}{4} \frac{B_1^2}{B_2} \sum_{n=1}^{\infty} a_n^2 k_n^4 J_o^2(k_n) + \frac{B_2}{8} \sum_{n=1}^{\infty} \sum_{m=1}^{\infty} \sum_{p=1}^{\infty} \sum_{q=1}^{\infty} a_n a_m a_p a_q \gamma_{nmpq}$$

$$+ e_o^2 B_2 \left[\sum_{n=1}^{\infty} a_n^2 J_o^2(k_n) + \sum_{n=1}^{\infty} \sum_{m=1}^{\infty} a_n a_m J_o(k_n) J_o(k_m) \right] + \frac{1}{4} B_2 B_3^2 B_o^2$$

$$- e_o B_1 \sum_{n=1}^{\infty} a_n^2 k_n^2 J_o^2(k_n) + \frac{B_1}{2} \sum_{n=1}^{\infty} \sum_{m=1}^{\infty} \sum_{p=1}^{\infty} a_n a_m a_p k_n^2 \tau_{nmp}$$

(3.57 Cont.)

$$- e_o B_2 \sum_{n=1}^{\infty} \sum_{m=1}^{\infty} \sum_{p=1}^{\infty} a_n a_m a_p \left[\tau_{nmp} - J_o(k_n) \alpha_{mp} \right]$$

$$- \frac{1}{2} B_2 B_3 B_o \sum_{n=1}^{\infty} \sum_{m=1}^{\infty} a_n a_m \alpha_{nm} - e_o 2 B_3 B_o \sum_{n=1}^{\infty} a_n J_o(k_n)$$

$$- \frac{(1 + \lambda_o + \mu)}{2} \left[(1 + \lambda_o)^2 - \mu^2 \right] \left[\frac{B_o}{1 + \lambda_o - \mu} \right.$$

$$- \frac{1}{2(1 + \lambda_o + \mu)} \sum_{n=1}^{\infty} \sum_{m=1}^{\infty} a_n a_m \phi_{nm}(1) \Bigg]^2$$

$$- \frac{1}{48} \left[12 \frac{B_1^2}{B_2} \left(\frac{1 + \lambda_o}{\mu} \right)^2 - \left(1 + \rho_o \right. \right.$$

(3.57)

$$\left. \left. + 12\lambda_o \frac{e^2}{h^2} \right) \right] \sum_{n=1}^{\infty} a_n^2 k_n^4 J_o^2(k_n) + \frac{Q}{2} \sum_{n=1}^{\infty} a_n J_o(k_n)$$

The expression for B_o is defined by

$$B_o = \frac{1 + \lambda_o}{1 + \lambda_o + \mu} \sum_{n=1}^{\infty} \sum_{m=1}^{\infty} a_n a_m \phi_{nm}(1) - \sum_{n=1}^{\infty} \sum_{m=1}^{\infty} a_n a_m \alpha_{nm}$$

(3.58)

$$- 2 e_o \sum_{n=1}^{\infty} a_n J_o(k_n) \ .$$

Quasi-Static Loading

By the principle of the stationary value of the total potential, the following relations must hold for static equilibrium:

$$\frac{1}{2} \frac{B_1^2}{B_2} a_n k_n^4 J_o^2(k_n) + \frac{B_2}{2} \sum_{m=1}^{\infty} \sum_{p=1}^{\infty} \sum_{q=1}^{\infty} a_m a_p a_q \gamma_{nmpq}$$

(3.59
Cont.)

$$+ 2 e_o^2 B_2 [a_n J_o^2(k_n) + J_o(k_n) \sum_{m=1}^{\infty} a_m J_o(k_m)]$$

$$+ B_2 B_3^2 B_o \left[\frac{1 + \lambda_o}{1 + \lambda_o + \mu} \sum_{m=1}^{\infty} a_m \phi_{nm}(1) - \sum_{m=1}^{\infty} a_m \alpha_{nm} - e_o J_o(k_n) \right]$$

$$- 2 e_o B_1 a_n k_n^2 J_o^2(k_n) + \frac{B_1}{2} [k_n^2 \sum_{m=1}^{\infty} \sum_{p=1}^{\infty} a_m a_p \tau_{nmp}$$

$$+ 2 \sum_{m=1}^{\infty} \sum_{p=1}^{\infty} a_m a_p k_m^2 \tau_{mnp}]$$

$$- e_o B_2 \left[\sum_{m=1}^{\infty} \sum_{p=1}^{\infty} a_m a_p \tau_{nmp} + 2 \sum_{m=1}^{\infty} \sum_{p=1}^{\infty} \tau_{mnp} \right.$$

(3.59
Cont.)

$$\left. - J_o(k_n) \sum_{m=1}^{\infty} \sum_{p=1}^{\infty} a_m a_p \alpha_{mp} - 2 \sum_{m=1}^{\infty} \sum_{p=1}^{\infty} a_m a_p J_o(k_m) \alpha_{np} \right]$$

$$- B_2 B_3 B_o \left[\sum_{m=1}^{\infty} a_m \alpha_{nm} + e_o J_o(k_n) \right]$$

$$- B_2 B_3 \left[\sum_{m=1}^{\infty} \sum_{p=1}^{\infty} a_m a_p \alpha_{mp} + 2 e_o \sum_{m=1}^{\infty} a_m J_o(k_m) \right] \left[\frac{1 + \lambda_o}{1 + \lambda_o + \mu} \sum_{m=1}^{\infty} a_m \phi_{nm}(1) \right.$$

$$\left. - \sum_{m=1}^{\infty} a_m \alpha_{nm} - e_o J_o(k_n) \right] - 2(1 + \lambda_o + \mu) [(1 + \lambda_o)^2 - \mu^2] \left\{ \frac{B_o}{1 + \lambda_o - \mu} \right.$$

$$- \frac{1}{2(1 + \lambda_o + \mu)} \sum_{m=1}^{\infty} \sum_{p=1}^{\infty} a_m a_p \phi_{mp}(1) \Bigg\} \Bigg\{ \frac{1}{1 + \lambda_o - \mu} \Bigg[\frac{1 + \lambda_o}{1 + \lambda_o - \mu} \sum_{m=1}^{\infty} a_m \phi_{nm}(1)$$

$$- \sum_{m=1}^{\infty} a_m \alpha_{nm} - e_o J_o(k_n) \Bigg] - \frac{1}{2(1 + \lambda_o + \mu)} \sum_{m=1}^{\infty} a_m \phi_{nm}(1) \Bigg\}$$

$$\text{(3.59)}$$

$$- \frac{1}{24} \Bigg[12 \frac{B_1^2}{B_2} \left(\frac{1 + \lambda_o}{\mu} \right)^2 - (1 + \rho_o + 12 \lambda_o \frac{e^2}{h^2}) \Bigg] a_n k_n^4 J_o^2(k_n)$$

$$+ \frac{Q}{2} J_o(k_n) = 0$$

where $n = 1, 2, 3, \ldots$.

Since the load, Q, becomes critical when the near static equilibrium point becomes unstable, then at Q_{cr} the following relation must hold:

$$\begin{vmatrix} \dfrac{\partial^2 U_T^*}{\partial a_1^2} & \dfrac{\partial^2 U_T^*}{\partial a_1 \partial a_2} & \cdots & \dfrac{\partial^2 U_T^*}{\partial a_1 \partial a_n} \\[2em] \dfrac{\partial^2 U_T^*}{\partial a_2 \partial a_1} & \dfrac{\partial^2 U_T^*}{\partial a_2^2} & \cdots & \dfrac{\partial^2 U_T^*}{\partial a_2 \partial a_n} \\ \vdots & \vdots & & \\ \dfrac{\partial^2 U_T^*}{\partial a_n \partial a_1} & \dfrac{\partial^2 U_T^*}{\partial a_n \partial a_2} & \cdots & \dfrac{\partial^2 U_T^*}{\partial a_n^2} \end{vmatrix} = 0 . \quad \text{(3.60)}$$

The simultaneous solution of the nonlinear algebraic set of Equations (3.59) and (3.60) yields Q_{cr} and its associated values of generalized coordinates, a_n.

Dynamic Step Loading

In this case the load, Q_D, is considered critical when the unstable equilibrium point is reached with zero kinetic energy thus giving a possibility of buckled motion. The critical load, $Q_{D_{cr}}$, is found by the simultaneous solution of Equations (3.59) and $U_T^* = 0$, with the additional requirement that the determinant in Equation (3.60) must be negative.

Impulsive Loading

For the case of the ideal impulse, it is assumed that the load is instantaneously converted into initial kinetic energy before any displacement occurs. If I_{mp} represents the impulse per unit mass, then

$$I_{mp} dm = \left(\frac{\partial w}{\partial t}\right)_i dm \qquad (3.61)$$

or

$$I_{mp} = \left(\frac{\partial w}{\partial t}\right)_i . \qquad (3.62)$$

The initial kinetic energy is

$$T_i = \int_o^R \int_o^{2\pi} \frac{\sigma h}{2} \left(\frac{\partial w}{\partial t}\right)_i^2 \; r dr d\theta \; ; \qquad (3.63)$$

$$T_i = \frac{\sigma h \pi R^2}{2} (I_{mp})^2 \; . \qquad (3.64)$$

The above expression, Equation (3.64), can be written in the following nondimensional form:

$$I_{mp}^* = (T_i^*)^{1/2} \qquad (3.65)$$

where

$$I_{mp}^* = \left[\frac{(1 - \mu^2)\sigma}{E}\right]^{1/2} \left(\frac{R}{h}\right)^2 I_{mp} \; . \qquad (3.66)$$

The impulse is considered to be critical when the zero-load unstable static equilibrium point is reached with zero kinetic energy. (See Equation 2.10.) Thus buckled motion is possible, and

$$I_{mp_{cr}}^* = \sqrt{U_{T_{cr}}^*} \qquad (3.67)$$

where $U_{T_{cr}}^*$ is the value of the total potential at the zero-load unstable static equilibrium point. This point is found by the simultaneous solution of Equations (3.59) with the load, Q, set equal to

zero. Since this is an unstable static equilibrium point, as in the dynamic step loading case, Equations (3.59) are solved subject to the condition that the value of the determinant in Equation (3.60) is negative.

CHAPTER IV

NUMERICAL SOLUTION AND RESULTS

The solutions to the three loading cases are obtained by taking
a finite number of terms in the series representation of the displace-
ment, w. Since the displacement is being represented by a finite
number of terms, these solutions are, of course, only approximate and
some estimate must be made of their range of applicability. Geometric
configurations corresponding to isotropic, lightly stiffened, moderately
stiffened and heavily stiffened geometries are considered. Lightly
stiffened geometry implies that most of the extensional stiffness is
provided by the thin skin. In a similar fashion, moderate stiffening
implies the extensional stiffnesses of the skin and stiffeners are of
the same order and heavy stiffening implies that most of the extensional
stiffness is provided by the stiffeners. The cases considered are
shown in Table 1.

Table 1. Geometric Configurations Considered

Amount of Stiffening	λ_o	ρ_o	Eccentricities Considered
Light	.222	5.0	$0, \pm 2, \pm 4, \pm 6$
Moderate	1.333	300.0	$0, \pm 4, \pm 8$
Heavy	2.667	2000.0	$0, \pm 4, \pm 8, \pm 12$

In order to have a consistent basis for comparison, it is convenient to introduce some new parameters. The classical critical pressure (quasi-static) for the complete sphere is

$$q_{cl} = \frac{2\ Eh^2}{\sqrt{3(1-\mu^2)}\ R_o^2} \ .$$

(4.1)

It is convenient to define the ratio

$$\rho_{cr} = \frac{q_{cr}}{q_{cl}}$$

(4.2)

where

$$q_{cr} = -\frac{Eh^4}{(1-\mu^2)R^4}\ Q_{cr} \ .$$

(4.3)

From the above expression and the fact that

$$R_o^2 = \frac{R^4}{4H^2}$$

(4.4)

the following relationship is obtained:

$$\rho_{cr} = -\frac{\sqrt{3(1-\mu^2)}}{8(1-\mu^2)}\ \left(\frac{h^2}{H^2}\right) Q_{cr} \ .$$

(4.5)

Furthermore, an initial rise parameter, λ, is introduced which is mathematically defined by

$$\lambda = 2[3(1 - \mu^2)]^{1/4} \left(\frac{H}{h_{eq}}\right)^{1/2} \qquad (4.6)$$

where h_{eq} is the sum of the shell thickness and the thickness corresponding to the volume of the stiffeners smeared uniformly about the midsurface of the cap. Neglecting the eccentricity of the stiffeners, the equivalent shell thickness is given by

$$h_{eq} = h(1 + \frac{A_r}{\ell_r h} + \frac{A_\theta}{\ell_\theta h}) \ . \qquad (4.7)$$

The deflected shape of the shell is represented approximately by taking one and two terms of the series, and the critical pressures and impulses desired are obtained by examining the total potential surface in the configuration space of the generalized coordinates a_1 and a_2. A family of potential surfaces is obtained. At $Q = 0$ the square root of the value of the total potential at the first unstable equilibrium point gives the critical impulse for the case of the ideal impulse. As the value (absolute) of the load is increased, the near stable and the unstable static equilibrium points approach each other and the level of the total potential at the unstable point decreases. At a value of the load, $Q_D = Q$, the level of the total

potential becomes zero at some unstable static equilibrium point for which a possible path exists and buckled motion is possible. This load represents the critical load for the case of dynamic step loading. As the absolute value of the load is increased, the near static equilibrium point becomes unstable and the corresponding load, $Q_{cr} = Q$, represents the critical load for the quasi-static case.

Numerical results for the three cases being studied were obtained by two methods, both involving extensive computer programming. For the ideal impulsive load a program was written which gave values of the total potential (at zero load) at closely spaced points in the configuration space for different values of the initial rise parameter, λ, for each geometric configuration. However, for the two remaining cases, a computer program was written which solved the nonlinear systems of equations indicated in Chapter III. The results obtained are presented in graphical form as load (or impulse) parameter versus initial rise parameter and are discussed separately in the following paragraphs.

The critical ratio, ρ_{cr}, for the quasi-static case was normalized using the results of Cole [2] for the complete sphere with a geometrical configuration similar to the shallow cap. The complete sphere results were those which corresponded to a load normal to the deflected midsurface during buckling and the normalized ratio was defined by the following mathematical relationship:

$$\rho^* = \frac{\rho_{cr}}{\rho_{cr_{sphere}}} \quad . \tag{4.8}$$

These normalizing factors are shown in the following table.

Table 2. Normalizing Factors for Quasi-static Loading

Geometrical Configuration	Eccentricity (e/h)	ρ_{cr} sphere
Isotropic	0	1.0
Light	0	2.9
	-2	4.9
	+2	4.0
	-4	8.2
	+4	6.2
	-6	11.3
	+6	9.2
Moderate	0	28.0
	-4	35.5
	+4	30.0
	-8	49.3
	+8	38.2
Heavy	0	90.6
	-4	96.9
	+4	90.6
	-8	109.0
	+8	96.0
	-12	126.0
	+12	107.0

The results for the quasi-static case are shown in Figures 5a, 5b and 5c with the normalized pressure ratio, $\rho*$, plotted versus the initial rise parameter, λ. The two-term solution is compared to the well-known solution of Budiansky [19], Thurston [25], Archer [26] and Weinitschke [27] to establish its validity. This comparison shows that the present solution is a good approximation for values of λ for which axisymmetric behavior prevails. For the range of λ-values considered, the data indicate that inside stiffeners (concave side) yield a stronger configuration than outside stiffeners. The fact that in Figure 5 the positive eccentricity curve lies above the negative is due solely to the fact that different normalizing factors were used ($\rho_{cr_{sphere}}$). In order to establish the true relationship between the buckling loads of the geometric configurations studied, the ratio $\rho*$ is multiplied by the appropriate normalizing factor from Table 2. Furthermore, the data indicate that the initial λ-value for which snap-through does occur, λ_{min}, increases as the eccentricity becomes larger. The critical curves ($\rho*$ versus λ) have the same characteristic shape for all geometric configurations considered. Based on a comparison between the present and the well accepted solution for the isotropic shell, it is thought that the results are valid for the portion of the curve contained between λ_{min} and $\rho* = 0.9$.

Figures 6a, 6b and 6c show the two-term solution obtained for the dynamic step loading case. The critical values obtained for the isotropic shell are in one to one correspondence with those derived by Simitses [9] using a similar computational procedure. Although
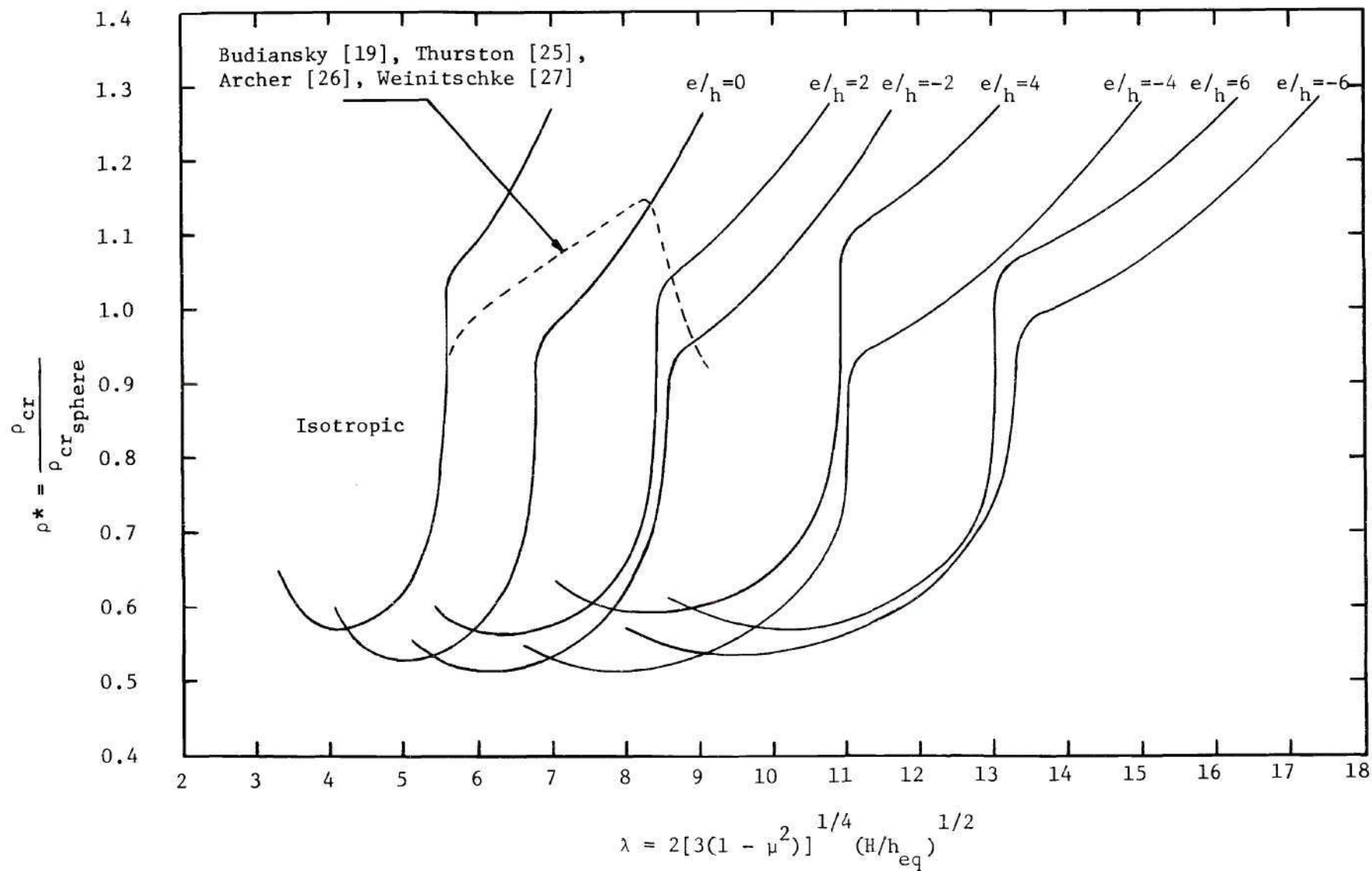
Figure 5a. Critical Buckling Ratio $\rho*$ versus Initial Rise Parameter, λ, for Quasi-static Loading (Isotropic and Light Stiffening).

The vertical axis is labeled $\rho* = \dfrac{\rho_{cr}}{\rho_{cr_{sphere}}}$

The horizontal axis is labeled $\lambda = 2[3(1 - \mu^2)]^{1/4} (H/h_{eq})^{1/2}$

Curve labels: Budiansky [19], Thurston [25], Archer [26], Weinitschke [27]; Isotropic; $e/h=0$; $e/h=2$; $e/h=-2$; $e/h=4$; $e/h=-4$; $e/h=6$; $e/h=-6$
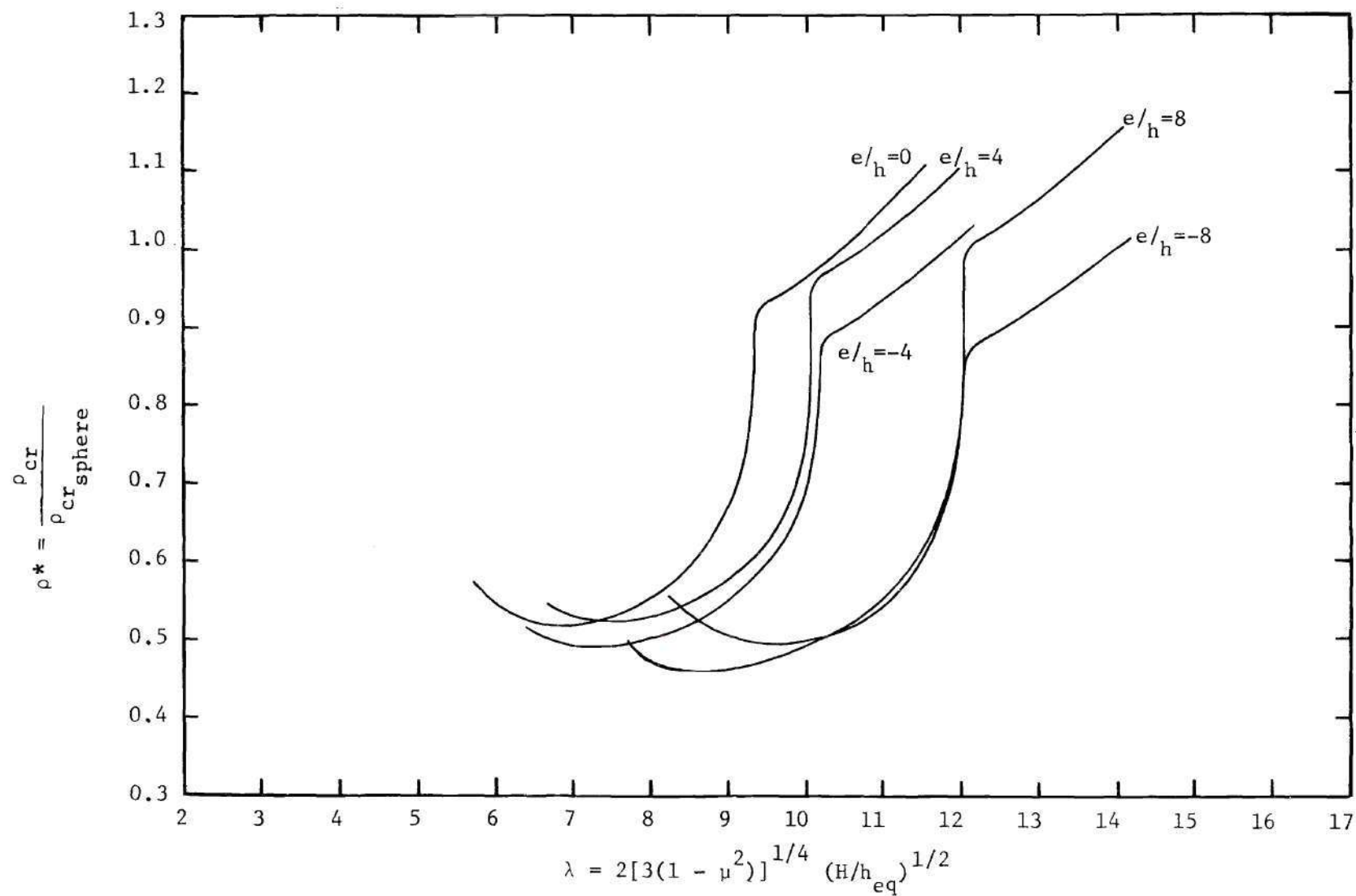
Figure 5b.   Critical Buckling Ratio $\rho*$ versus Initial Rise Parameter, λ, for Quasi-static Loading (Moderate Stiffening).
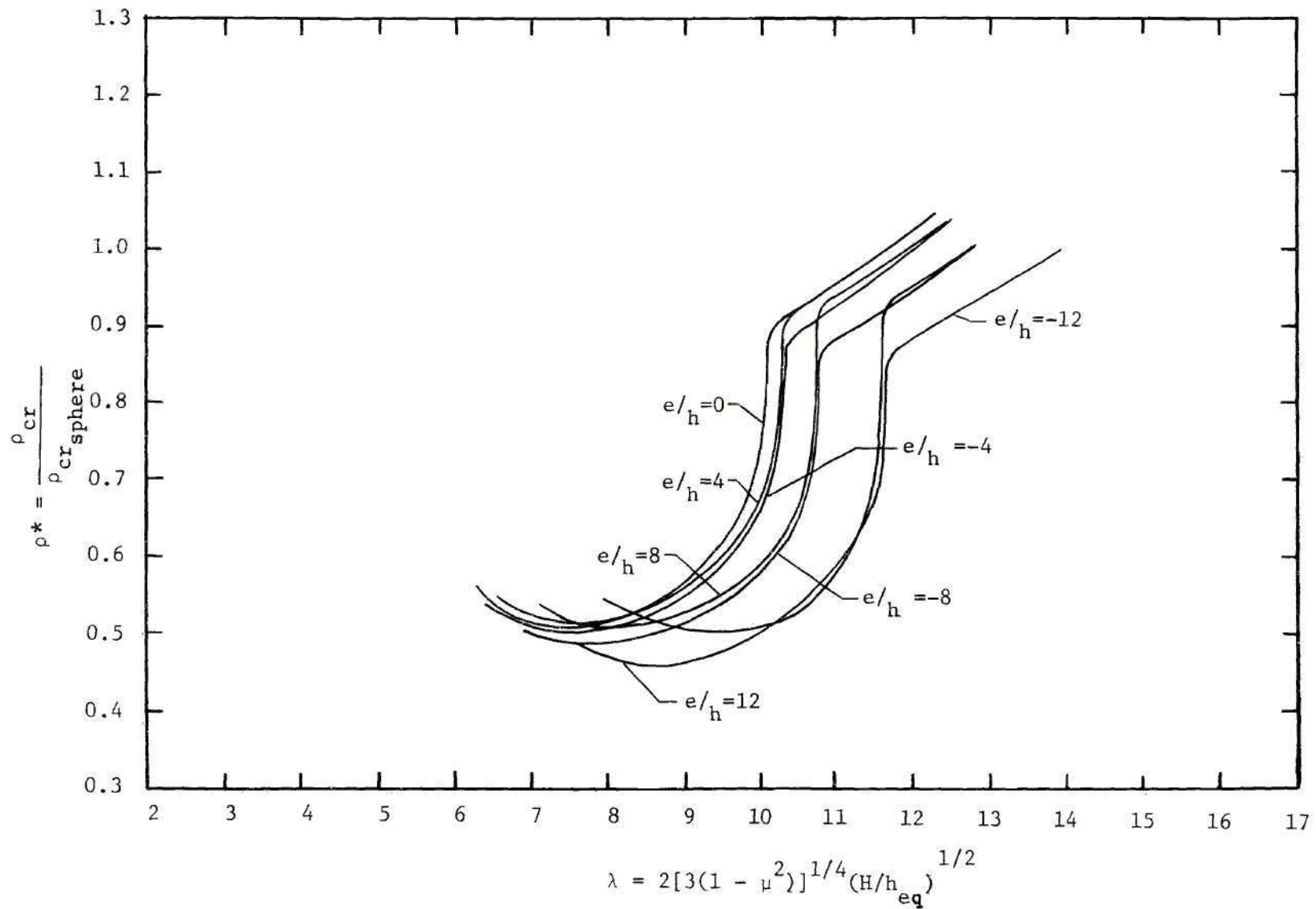
Figure 5c.   Critical Buckling Ratio ρ^* versus Initial Rise Parameter, λ, for Quasi-static Loading (Heavy Stiffening).

The horizontal axis is $\lambda = 2[3(1 - \mu^2)]^{1/4}(H/h_{eq})^{1/2}$

The vertical axis is $\rho^* = \dfrac{\rho_{cr}}{\rho_{cr_{sphere}}}$

Curve labels: $e/_h = -12$, $e/_h = 0$, $e/_h = -4$, $e/_h = 4$, $e/_h = 8$, $e/_h = -8$, $e/_h = 12$
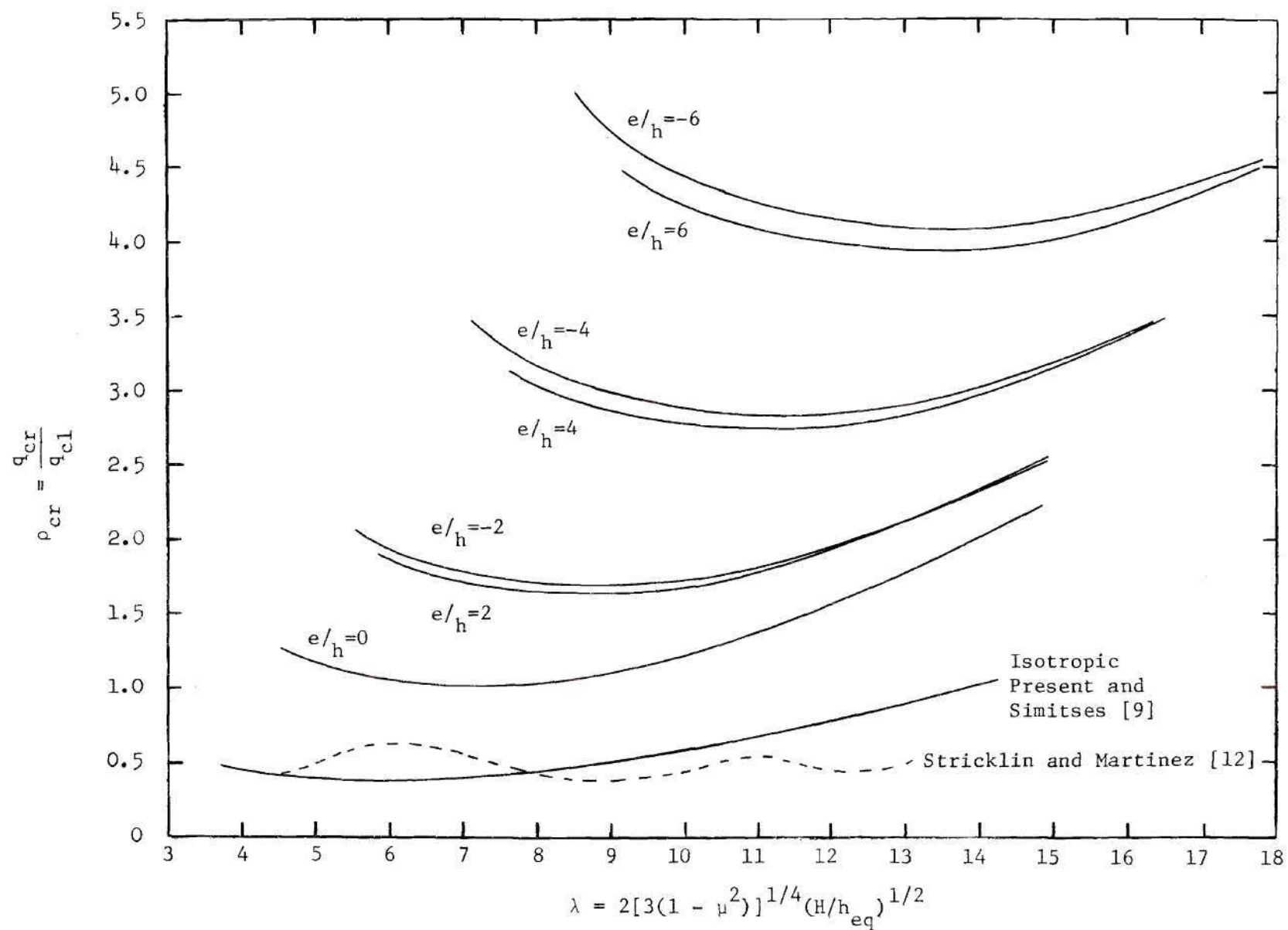
Figure 6a. Buckling Ratio ρ_{cr} versus Initial Rise Parameter, λ, for Dynamic Loading (Isotropic and Light Stiffening).

The vertical axis is labeled $\rho_{cr} = \dfrac{q_{cr}}{q_{cl}}$ with values from 0 to 5.5.

The horizontal axis is labeled $\lambda = 2[3(1 - \mu^2)]^{1/4}(H/h_{eq})^{1/2}$ with values from 3 to 18.

Curves are labeled $e/h=-6$, $e/h=6$, $e/h=-4$, $e/h=4$, $e/h=-2$, $e/h=2$, $e/h=0$, Isotropic Present and Simitses [9], and Stricklin and Martinez [12].
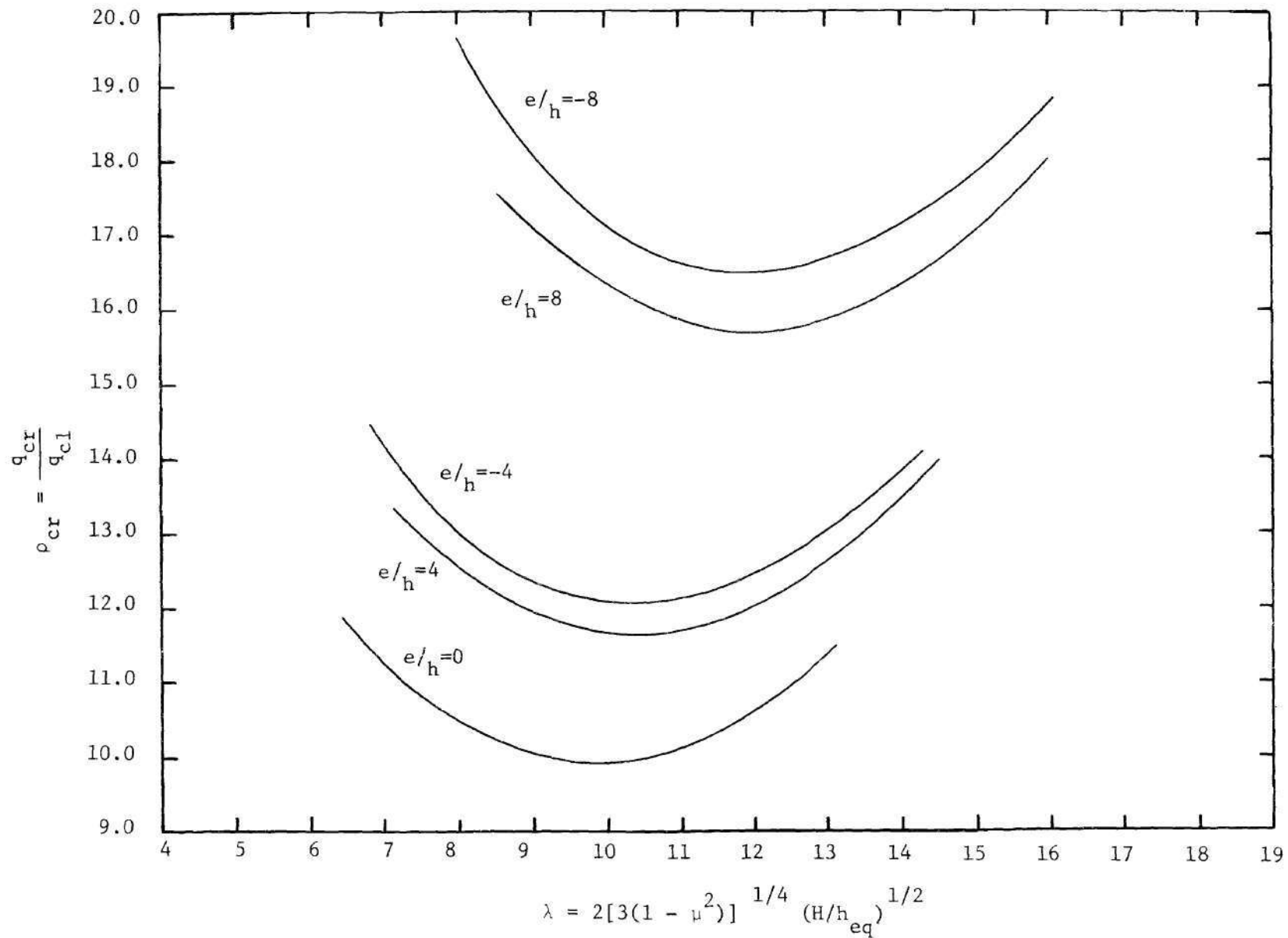
Figure 6b. Buckling Ratio ρ_{cr} versus Initial Rise Parameter, λ, for Dynamic Loading (Moderate Stiffening).
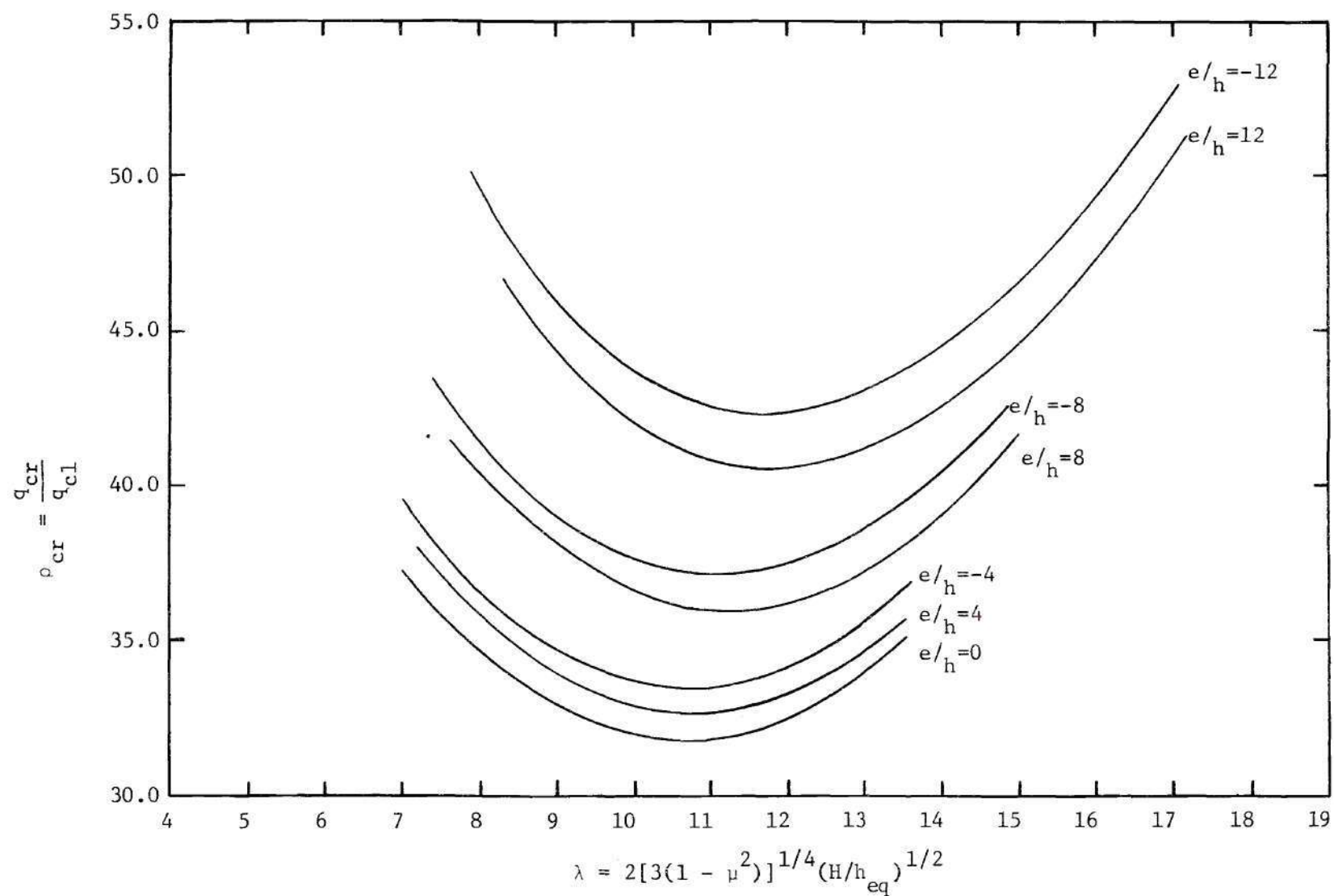
Figure 6c. Buckling Ratio ρ_{cr} versus Initial Rise Parameter, λ, for Dynamic Loading (Heavy Stiffening).

The figure plots $\rho_{cr} = \dfrac{q_{cr}}{q_{cl}}$ (vertical axis, from 30.0 to 55.0) against $\lambda = 2[3(1 - \mu^2)]^{1/4}(H/h_{eq})^{1/2}$ (horizontal axis, from 4 to 19). Curves are labeled $e/h=-12$, $e/h=12$, $e/h=-8$, $e/h=8$, $e/h=-4$, $e/h=4$, and $e/h=0$.

Stricklin and Martinez [12], Stephens and Fulton [11] and Huang [13] have data for a similar problem direct comparison is not practical because they sought to derive a precise value of the instability load whereas the objective of this thesis was solely to compute the lower possible bound. The apparent anomaly between the values of bound established for $\lambda > 7.8$ and the computation of Stricklin and Martinez [12] is related to the point made strongly in the penultimate paragraph of Chapter II viz. that a two degree of freedom system is not necessarily in all circumstances a good approximation to a continuous system.

Although the data presented in graphic form indicate that the influence of eccentricity changes at a specific λ it is nevertheless concluded that inside stiffeners yield the stronger configuration. This conclusion hinges on the fact that the two-term solution is not considered accurate for the higher values of λ. The results also show that the initial λ-value for which dynamic snap-through is possible increases as the value of eccentricity becomes larger.

In Figures 7a, 7b, 7c and 7d, critical impulses are plotted versus the initial rise parameter, λ. The isotropic solution is compared with those of Budiansky and Roth [7], Humphreys and Bodner [6] and Simitses [9] and it is seen from the graphic display that within the range of λ-values considered appropriate that a lower bound is certainly established.

The results for the stiffened geometries indicate that, contrary to the other two cases considered, outside stiffeners yield the stronger
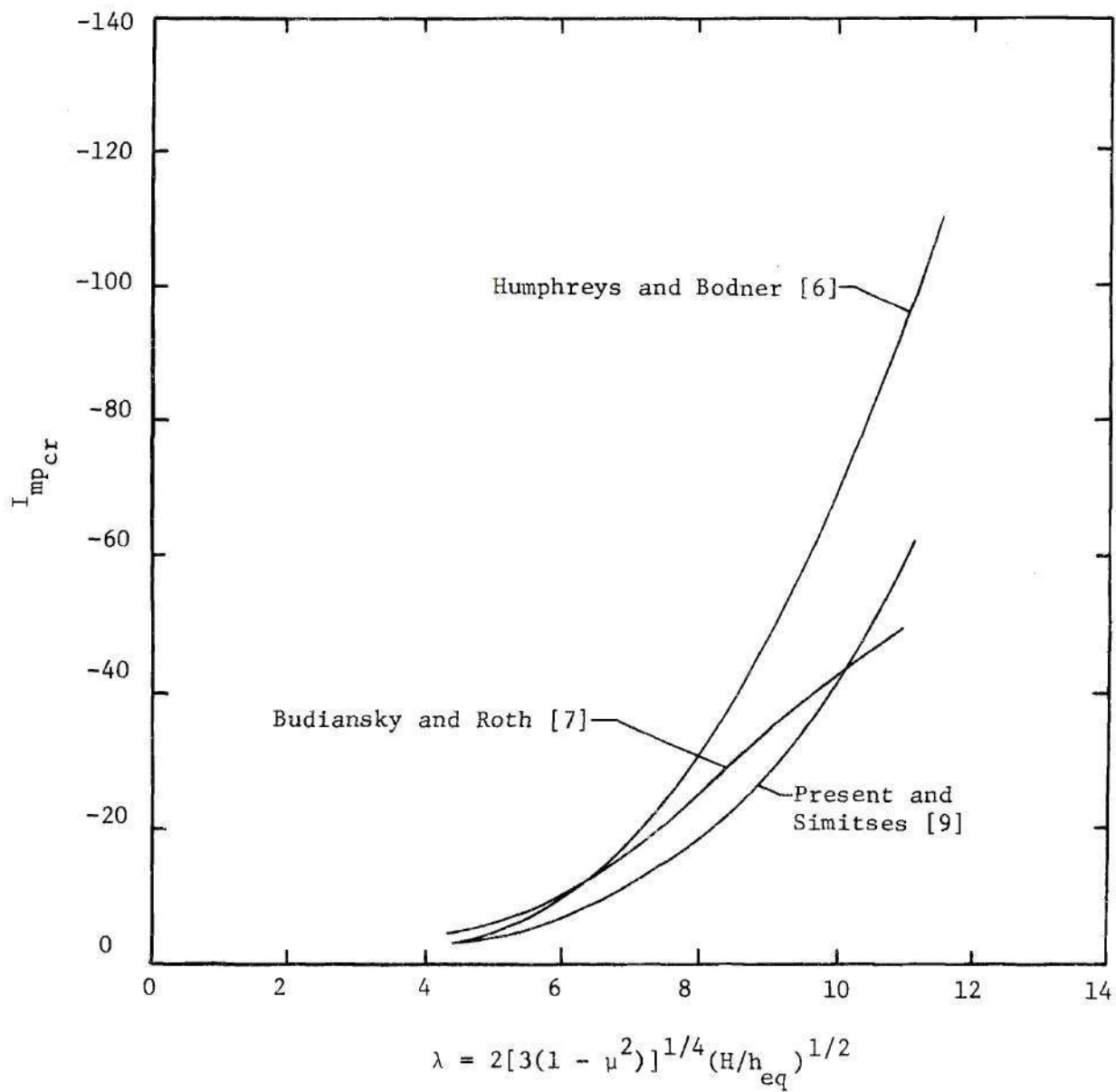
Figure 7a. Critical Impulse versus Initial Rise Parameter, λ (Isotropic).

The figure axes and labels:

- Vertical axis: $I_{mp_{cr}}$ with values 0, -20, -40, -60, -80, -100, -120, -140.
- Horizontal axis: 0, 2, 4, 6, 8, 10, 12, 14.
- Horizontal axis label: $\lambda = 2[3(1 - \mu^2)]^{1/4}(H/h_{eq})^{1/2}$

Curve labels:
- Humphreys and Bodner [6]
- Budiansky and Roth [7]
- Present and Simitses [9]
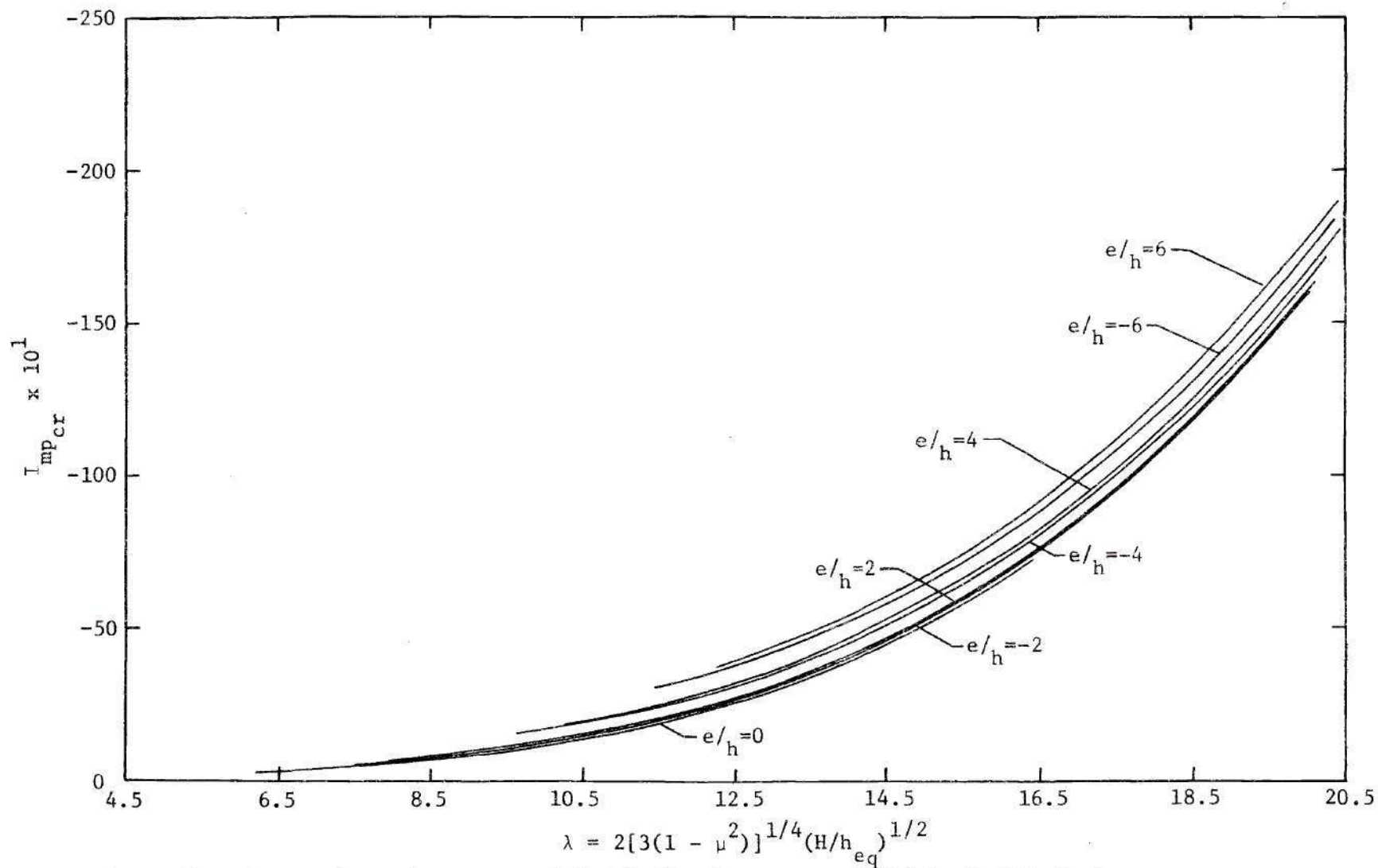
Figure 7b.   Critical Impulse versus Initial Rise Parameter, λ (Light Stiffening).

The plot axes: vertical axis labeled $I_{mp_{cr}} \times 10^1$ ranging from 0 to -250; horizontal axis labeled $\lambda = 2[3(1 - \mu^2)]^{1/4}(H/h_{eq})^{1/2}$ ranging from 4.5 to 20.5. Curves labeled $e/_h = 6$, $e/_h = -6$, $e/_h = 4$, $e/_h = 2$, $e/_h = -4$, $e/_h = -2$, $e/_h = 0$.
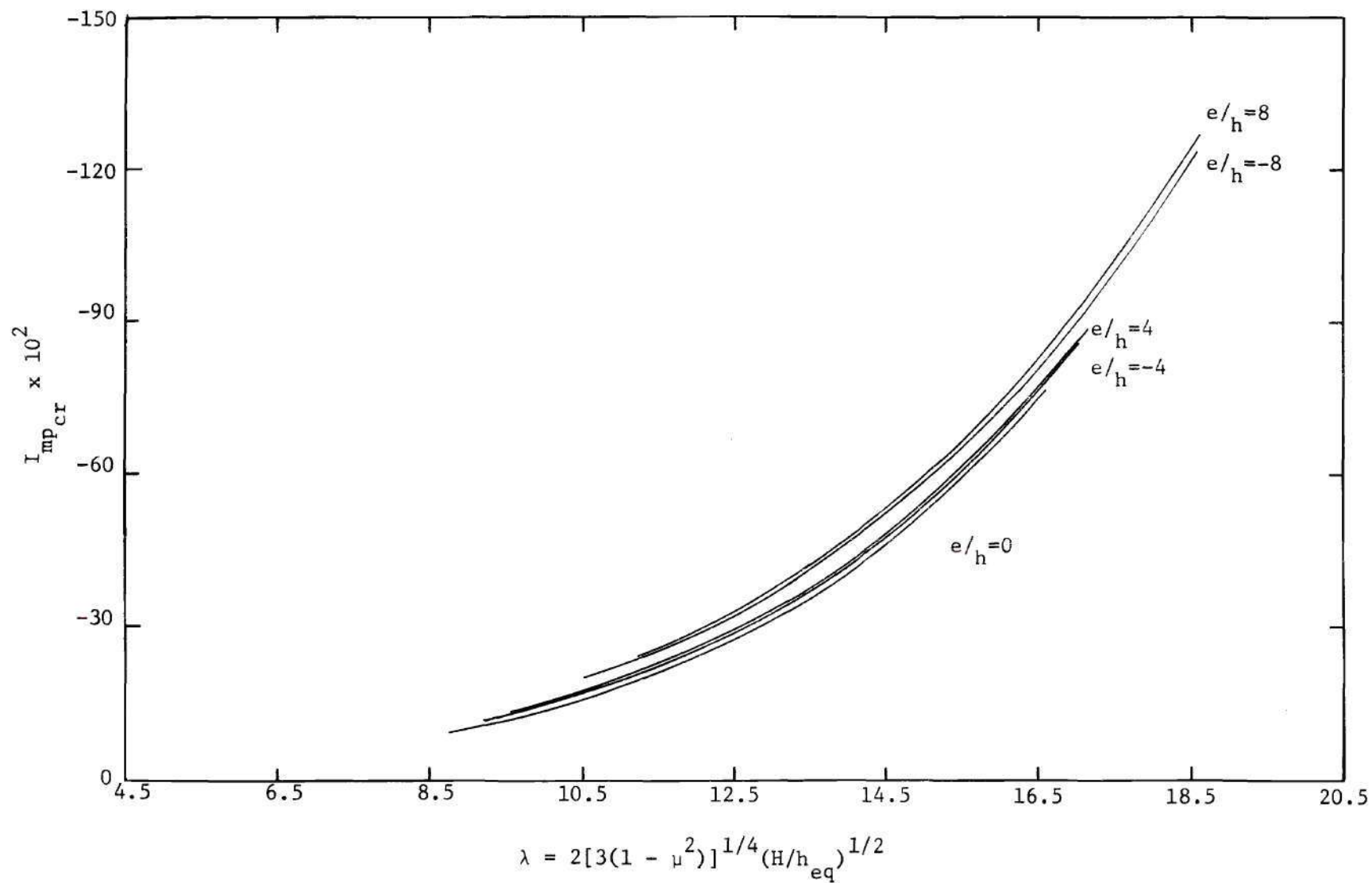
Figure 7c. Critical Impulse versus Initial Rise Parameter, λ (Moderate Stiffening).

The y-axis is labeled $I_{mp_{cr}} \times 10^2$ with values -150, -120, -90, -60, -30, 0.

The x-axis is labeled $\lambda = 2[3(1 - \mu^2)]^{1/4}(H/h_{eq})^{1/2}$ with values 4.5, 6.5, 8.5, 10.5, 12.5, 14.5, 16.5, 18.5, 20.5.

Curves labeled $e/_h=8$, $e/_h=-8$, $e/_h=4$, $e/_h=-4$, $e/_h=0$.
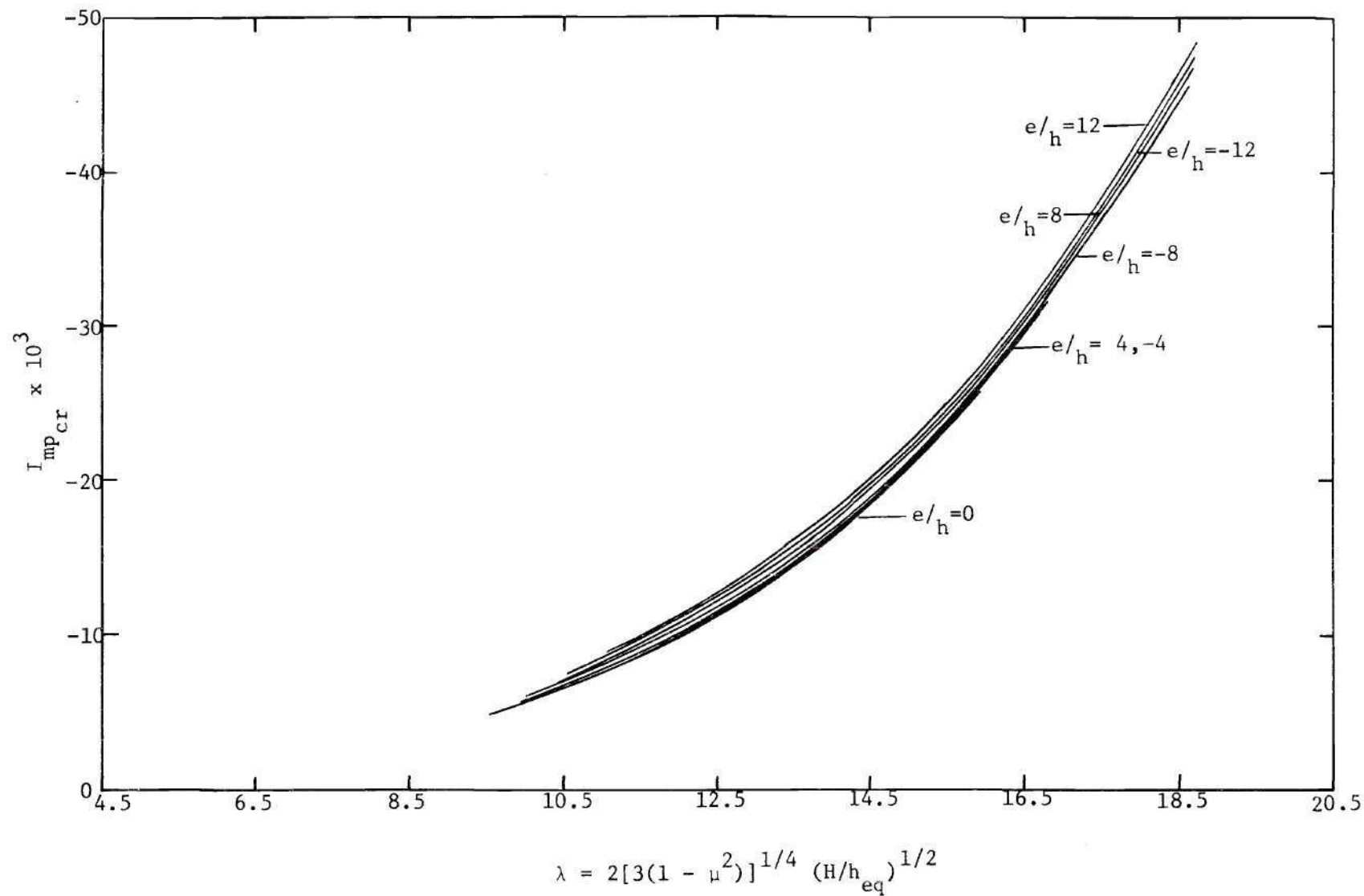
Figure 7d. Critical Impulse versus Initial Rise Parameter, λ (Heavy Stiffening).

The figure's vertical axis is labeled $I_{mp_{cr}} \times 10^3$ with values from 0 to -50. The horizontal axis ranges from 4.5 to 20.5 and is labeled:

$$\lambda = 2[3(1 - \mu^2)]^{1/4} (H/h_{eq})^{1/2}$$

Curve labels: $e/h = 12$, $e/h = -12$, $e/h = 8$, $e/h = -8$, $e/h = 4, -4$, $e/h = 0$.

configuration. However, this effect is very small.

In a recent paper Huang [13] stated that for the ideal impulse snap-through is not possible for the continuous system. He based this conclusion on the fact that for times $t > 0$ no load is present and there is only one possible static equilibrium position for the shell, the undeformed shape. The method used in the present work indicates that snap-through due to impulse loading is possible for the two degree of freedom system studied. The potential surfaces obtained indicate a possible path from the near static equilibrium point (undeformed position) through an unstable equilibrium point to a far stable equilibrium point. However, the static unstable equilibrium point and the far static stable equilibrium points are very close to one another in the configuration space and are almost identical in energy level. Also, the values of the generalized coordinates, a_1 and a_2, obtained at the unstable static equilibrium point indicate that a very large deflection is needed before snap-through occurs. The deflection at the center of the cap indicated by these two coordinates is greater than the initial rise of the cap, H. In Figure 8 these coordinates are plotted versus the initial rise parameter for one specified geometrical configuration. This curve is typical of all geometrical configurations considered.
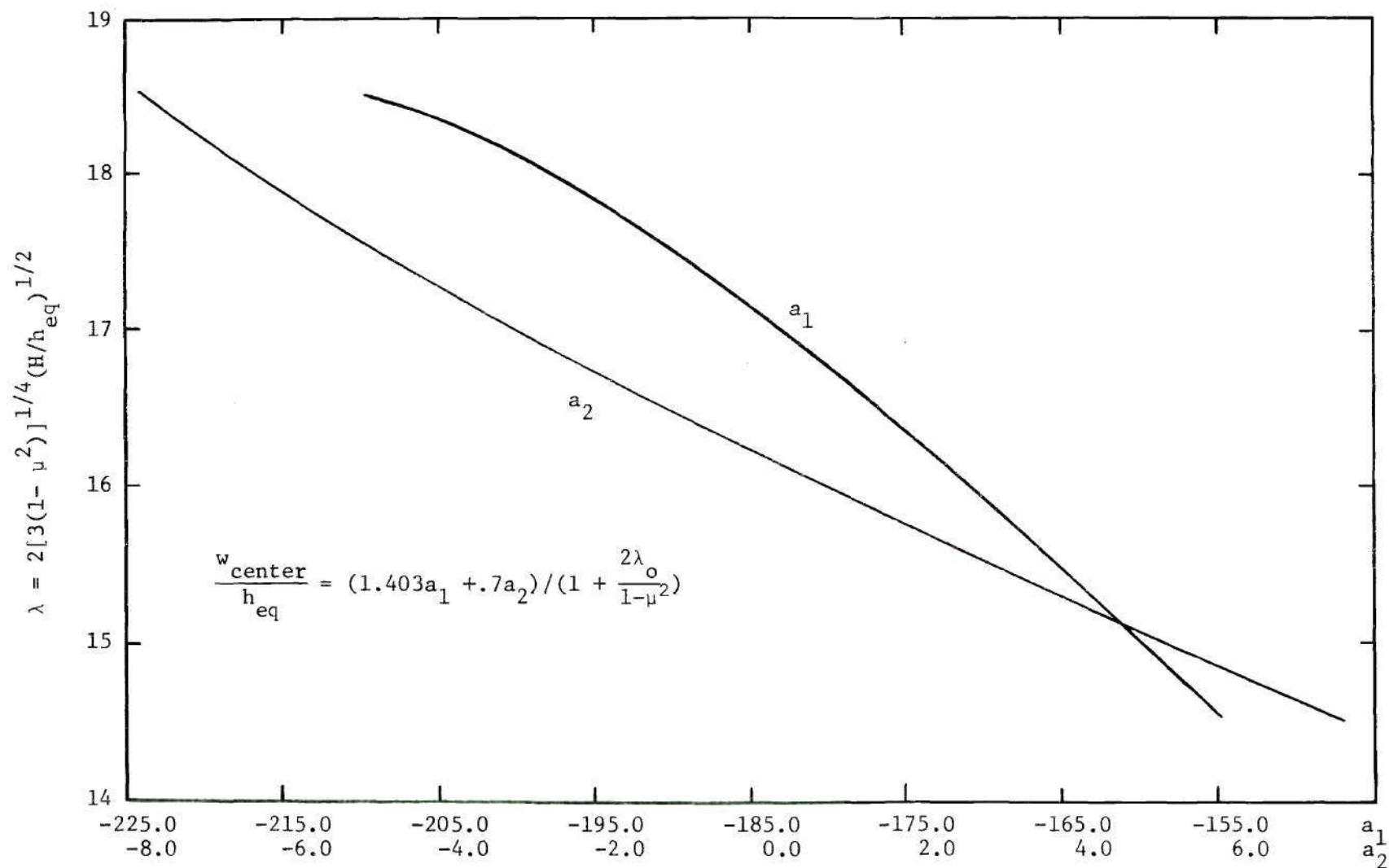
Figure 8. Sample Generalized Coordinates for Impulse Loading (Moderate Stiffening, $e/_h = 8$).

The vertical axis is labeled:
$$\lambda = 2[3(1-\mu^2)]^{1/4}(H/h_{eq})^{1/2}$$

The equation shown in the plot:
$$\frac{w_{center}}{h_{eq}} = (1.403a_1 + .7a_2)/(1 + \frac{2\lambda_o}{1-\mu^2})$$

The horizontal axis is labeled a_1 over a_2.

CHAPTER V

CONCLUSIONS AND RECOMMENDATIONS

Snap-through buckling of shallow spherical caps is possible under dynamic step loading. For the ideal impulse, buckling is possible if a far stable equilibrium point exists.

By studying the generated data, the following important conclusions are drawn:

1) Eccentricity of the stiffeners has a definite effect on the critical pressures of shallow caps.

2) Inside stiffeners yield a stronger configuration for both quasi-static and dynamic step loading conditions for which the two-term solution is valid.

3) For the same geometrical configuration the critical pressure is lower for a dynamic load than for a quasi-static load.

4) For the ideal impulse, outside stiffeners yield the stronger configuration but the eccentricity effect is very small.

5) In all cases, buckling is possible for λ-values higher than some minimum. The minimum value is approximately 3.2 for the isotropic configuration and increases as the value of eccentricity becomes larger.

Additional work on eccentrically stiffened shells is desirable. In particular, further attention should be paid to the problems

associated with various boundary conditions and the validity of the smear process should be critically examined. An effort should be made to extend the restricted λ range by asymmetric deformations. Finally, a study of the influence of other spatial load distributions should be made with particular emphasis being directed toward asymmetric distributions.

APPENDIX A

INTEGRATION OF THE COMPATIBILITY EQUATION

The compatibility equation for an eccentrically stiffened
shallow spherical cap under the assumption of rotationally symmetric
deformations and initial shape $z = z(r)$ is as follows:

$$(1 + \lambda_o) \, \nabla^4 \psi = e\lambda_o \mu E^p \nabla^4 w - E^p [(1 + \lambda_o)^2 - \mu^2] \ .$$

$$(A.1)$$

$$\left[\frac{w,_r}{r} z,_{rr} + \frac{w,_r}{r} w,_{rr} + \frac{z,_r}{r} w,_{rr} \right]$$

where

$$\nabla^4 = \frac{d^4}{dr^4} + \frac{2}{r} \frac{d^3}{dr^3} - \frac{1}{r^2} \frac{d^2}{dr^2} + \frac{1}{r^3} \frac{d}{dr} \ . \qquad (A.2)$$

The constants α_o and β_o are defined by the equations

$$\alpha_o = e\left(\frac{\lambda_o}{1 + \lambda_o}\right) \mu \, E^p \ ; \qquad (A.3)$$

$$\beta_o = \frac{E^p}{1 + \lambda_o} \, [(1 + \lambda_o)^2 - \mu^2] \ . \qquad (A.4)$$

It is noted that ∇^4 may be written in the form

$$\nabla^4 = \frac{1}{r} \frac{d}{dr} \left\{ r \frac{d}{dr} \left[\frac{1}{r} \frac{d}{dr} \left(r \frac{d}{dr} \right) \right] \right\}. \tag{A.5}$$

The compatibility equation can then be written as

$$\frac{1}{r} \frac{d}{dr} \left\{ r \frac{d}{dr} \left[\frac{1}{r} \frac{d}{dr} \left(r \frac{d}{dr} \right) \right] \right\} \psi = \alpha_o \frac{1}{r} \frac{d}{dr} \left\{ r \frac{d}{dr} \left[\frac{1}{r} \frac{d}{dr} \left(r \frac{d}{dr} \right) \right] \right\} w$$

$$- \frac{\beta_o}{r} \left[\frac{dw}{dr} \left(\frac{d^2 z}{dr^2} + \frac{d^2 w}{dr^2} \right) + \frac{dz}{dr} \frac{d^2 w}{dr^2} \right] . \tag{A.6}$$

Assuming that the undeformed meridional curve is approximated by a parabola, the following may be written

$$z = H \left[1 - \left(\frac{r}{R} \right)^2 \right]; \tag{A.7}$$

$$\frac{dz}{dr} = - \frac{2H}{R^2} r ; \tag{A.8}$$

$$\frac{d^2 z}{dr^2} = - \frac{2H}{R^2} . \tag{A.9}$$

The substitutions of the above equations into Equation (A.6) give the

following expression for the compatibility equation

$$\frac{1}{r}\frac{d}{dr}\left\{r\frac{d}{dr}\left[\frac{1}{r}\frac{d}{dr}\left(r\frac{d\psi}{dr}\right)\right]\right\} = \frac{\alpha_o}{r}\frac{d}{dr}\left\{r\frac{d}{dr}\left[\frac{1}{r}\frac{d}{dr}\left(r\frac{dw}{dr}\right)\right]\right\}$$

(A.10)

$$+ \beta_o \frac{2H}{R^2}\left(\frac{1}{r}\right)\left[\frac{dw}{dr} + r\frac{d^2w}{dr^2} - \frac{R^2}{2H}\frac{dw}{dr}\frac{d^2w}{dr^2}\right] .$$

The relationship between ψ and w may be found by four straightforward integrations between the limits 0 and r. These integrations give the following expression

$$\psi = \alpha_o w + \beta_o \frac{2H}{R^2}\int_o^r \frac{1}{y}\int_o^y xwdxdy - \frac{\beta_o}{2}\int_o^r \frac{1}{s}\int_o^s y\int_o^y \frac{1}{x}\left(\frac{dw}{dx}\right)^2 dxdyds$$

(A.11)

$$+ C_1\frac{r^2}{4}(\ell n r - 1) + C_2\frac{r^2}{4} + C_3 \ell n r + C_4 .$$

Now, by requiring the stresses

$$N_r = \frac{1}{r}\psi,_r ;$$

(A.12)

$$N_\theta = \psi,_{rr}$$

to be finite at $r = 0$ it can easily be shown that the constants C_1 and C_3 must be 0. Furthermore, using the boundary condition at $r = R$

relating the stress function to the spatial derivative of the normal displacement

$$\psi,_{rr} - \frac{\mu}{1 + \lambda_o} \frac{\psi,_r}{R} = \alpha_o w,_{rr} \tag{A.13}$$

along with the boundary conditions

$$w = 0 \; ; \tag{A.14}$$

$$w,_r = 0 \tag{A.15}$$

the value of the constant, C_2, may be found and is given by

$$C_2 = \left(\frac{1 + \lambda_o + \mu}{1 + \lambda_o - \mu} \right) \beta_o \left[\frac{4H}{R^4} \int_o^R rw dr \right. \tag{A.16}$$

$$\left. + \left(\frac{1 + \lambda_o}{1 + \lambda_o + \mu} \right) \int_o^R \frac{1}{r} \left(\frac{dw}{dr} \right)^2 dr - \frac{1}{R^2} \int_o^R r \int_o^r \frac{1}{x} \left(\frac{dw}{dx} \right)^2 dx dr \right] .$$

Finally, the relationship between the stress function, ψ, and the normal displacement, w, may be written as

$$\psi = \alpha_o w + \beta_o \frac{2H}{R^2} \int_o^r \frac{1}{y} \int_o^y xw dx dy - \frac{\beta_o}{2} \int_o^r \frac{1}{s} \int_o^s y \int_o^y \frac{1}{x} \left(\frac{dw}{dx} \right)^2 dx dy ds$$

$$+ r^2 \left(\frac{1 + \lambda_o + \mu}{1 + \lambda_o - \mu} \right) \frac{\beta_o}{4} \left[\frac{4H}{R^4} \int_o^R rwdr + \left(\frac{1 + \lambda_o}{1 + \lambda_o + \mu} \right) \int_o^R \frac{1}{r} \left(\frac{dw}{dr} \right)^2 dr \right.$$

$$\left. - \frac{1}{R^2} \int_o^R r \int_o^r \left(\frac{dw}{dx} \right)^2 dxdr \right] + C_4$$

$$(A.17)$$

where C_4 is an undetermined constant whose value is of no consequence since only derivatives of ψ will be used.

APPENDIX B

THE STRAIN ENERGY FUNCTION

In this Appendix the strain energy U, is derived for rotationally symmetric deformations in a form in which it is a function of the geometrical configuration, structural properties and the normal displacement, w.

The strain energy, U, is written as

$$U = 2\pi \int_{0}^{R} \frac{1}{2} (N_r \varepsilon_{rr} + N_\theta \varepsilon_{\theta\theta} + M_r \kappa_{rr} + M_\theta \kappa_{\theta\theta}) r dr. \qquad (B.1)$$

The constitutive relations

$$(E^P + E^S)\varepsilon_{rr} + \mu E^P \varepsilon_{\theta\theta} + eE^S \kappa_{rr} = N_r \quad ; \qquad (B.2)$$

$$\mu E^P \varepsilon_{rr} + (E^P + E^S)\varepsilon_{\theta\theta} + eE^S \kappa_{\theta\theta} = N_\theta \qquad (B.3)$$

are employed to solve for the strains ε_{rr} and $\varepsilon_{\theta\theta}$.

$$\varepsilon_{rr} = \frac{(E^P + E^S)N_r - \mu E^P N_\theta - eE^S[(E^P + E^S)\kappa_{rr} - \mu E^P \kappa_{\theta\theta}]}{(E^P)^2 [(1 + \lambda_o)^2 - \mu^2]} \qquad (B.4)$$

$$\varepsilon_{\theta\theta} = \frac{-\mu E^P N_r + (E^P + E^S)N_\theta - eE^S[-\mu E^P \kappa_{rr} + (E^P + E^S)\kappa_{\theta\theta}]}{(E^P)^2 [(1 + \lambda_o)^2 - \mu^2]} \ . \tag{B.5}$$

The moment-curvature relations are

$$M_r = (D + D^S + E^S e^2)\kappa_{rr} + \mu D\kappa_{\theta\theta} + E^S e\varepsilon_{rr} \ ; \tag{B.6}$$

$$M_\theta = \mu D\kappa_{rr} + (D + D^S + E^S e^2)\ \kappa_{\theta\theta} + E^S e\varepsilon_{\theta\theta} \ . \tag{B.7}$$

Substitution of Equations (B.4), (B.5), (B.6) and (B.7) into Equation (B.1) gives

$$U = \pi \int_o^R \left[\!\!\left[\frac{1}{(E^P)^2 [(1 + \lambda_o)^2 - \mu^2]} \left\{ (E^P + E^S)(N_r^2 + N_\theta^2) - 2\mu E^P N_r N_\theta \right.\right.$$

$$- eE^S[N_r(E^P + E^S)\kappa_{rr} - N_r \mu E^P \kappa_{\theta\theta} - N_\theta \mu E^P \kappa_{rr} \tag{B.8}$$

$$\left. + N_\theta(E^P + E^S)\kappa_{\theta\theta}] \right\} + (D + D^S + E^S e^2)(\kappa_{rr}^2 + \kappa_{\theta\theta}^2)$$

$$\left. + 2\mu D\kappa_{\theta\theta}\kappa_{rr} + eE^S(\varepsilon_{rr}\kappa_{rr} + \varepsilon_{\theta\theta}\kappa_{\theta\theta}) \right]\!\!\right] rdr.$$

Further substitution of Equations (B.4) and (B.5) into Equation (B.8)

and algebraic manipulation gives

$$U = \pi \int_o^R \left[\left[\frac{1}{(E^P)^2 \left[(1 + \lambda_o)^2 - \mu^2\right]} \left\{ (E^P + E^S)(N_r^2 + N_\theta^2) \right.\right.\right.$$

$$- 2 \mu E^P N_r N_\theta - (eE^S)^2 \left[(E^P + E^S)(\kappa_{rr}^2 + \kappa_{\theta\theta}^2)\right.$$

$$\left.\left. - 2 \mu E^P \kappa_{rr} \kappa_{\theta\theta}\right]\right\} + (D + D^S + E^S e^2)(\kappa_{rr}^2 + \kappa_{\theta\theta}^2)$$

$$\left.\left. + 2 \mu D \kappa_{rr} \kappa_{\theta\theta} \right]\right] r dr .$$

(B.9)

The expressions

$$\kappa_{rr} = - w,_{rr} \quad ;$$

$$\kappa_{\theta\theta} = - \frac{w,_r}{r}$$

(B.10)

and

$$N_\theta = \psi,_{rr} \quad ;$$

$$N_r = \frac{\psi,_r}{r}$$

(B.11)

are substituted into Equation (B.9) to give the strain energy function,

U, in terms of the normal displacement, w, and the stress function, ψ.

$$U = \pi \int_0^R \left[\!\!\left[\frac{1}{E^p[(1 + \lambda_o)^2 - \mu^2]} \left\{ (1 + \lambda_o)(\psi,_{rr}^2 + \frac{1}{r^2} \psi,_r^2) \right.\right.\right.$$

$$\left. -2\mu \frac{\psi,_r \psi,_{rr}}{r} - (eE^s)^2 [(1 + \lambda_o)(w,_{rr}^2 + \frac{1}{r^2} w,_r^2) - 2\mu \frac{w,_r w,_{rr}}{r}] \right\}$$

$$\left.\left. + D[1 + \rho_o + 12 \lambda_o (\frac{e}{h})^2] (w,_{rr}^2 + \frac{1}{r^2} w,_r^2) + 2\mu D \frac{w,_r w,_{rr}}{r} \right]\!\!\right] rdr \qquad (B.12)$$

Equation (B.12) may be rewritten in the following form

$$U = \pi \int_0^R \left[\!\!\left[\frac{1 + \lambda_o}{E^p[(1 + \lambda_o)^2 - \mu^2]} \left\{ (\frac{\psi,_r}{r} + \psi,_{rr})^2 - 2\left(\frac{1 + \lambda_o + \mu}{1 + \lambda_o}\right) \frac{\psi,_r}{r} \psi,_{rr} \right.\right.\right.$$

$$\left. - (eE^s)^2 \left[(\frac{w,_r}{r} + w,_{rr})^2 - 2\left(\frac{1 + \lambda_o + \mu}{1 + \lambda_o}\right) \frac{w,_r}{r} w,_{rr} \right] \right.$$

$$\qquad (B.13)$$

$$\left. + D \left[1 + \rho_o + 12 \lambda_o \frac{e^2}{h^2} \right] (\frac{w,_r}{r} + w,_{rr})^2 \right.$$

$$\left.\left. - 2D \left[1 - \mu + \rho_o + 12 \lambda_o \frac{e^2}{h^2} \right] \frac{w,_r}{r} w,_{rr} \right]\!\!\right] rdr .$$

The relations

$$\int_o^R w,_r w,_{rr} \, dr = 0$$

and

$$\int_o^R \psi,_r \psi,_{rr} \, dr = \frac{(\psi,_r)^2}{2} \Bigg|_o^R$$

are used in order to write the strain energy in the form below

$$U = \frac{\pi(1 + \lambda_o)}{E^P[(1 + \lambda_o)^2 - \mu^2]} \int_o^R (\psi,_{rr} + \frac{\psi,_r}{r})^2 \, r \, dr$$

$$- \pi \left\{ \frac{(eE^s)^2(1 + \lambda_o)}{E^P[(1 + \lambda_o)^2 - \mu^2]} - D(1 + \rho_o + 12\lambda_o \frac{e^2}{h^2}) \right\} \int_o^R (w,_{rr} + \frac{w,_r}{r})^2 \, r \, dr$$

<div align="right">(B.14)</div>

$$- \frac{\pi(1 + \lambda_o + \mu)}{E^P[(1 + \lambda_o)^2 - \mu^2]} (\psi,_r)^2 \Bigg|_o^R \, .$$

Using the relationship between ψ and w established in Appendix A the following expressions are derived:

$$(\psi,_{rr} + \frac{\psi,_r}{r})^2 = \alpha_o^2 (w,_{rr} + \frac{w,_r}{r})^2 + \frac{\beta_o^2}{4} (\int_o^r \frac{w,_x}{x} \, dx)^2 \tag{B.15}$$

$$+ \left(\frac{2H\beta_o w}{R^2}\right)^2 + C_o^2$$

$$+ (w,_{rr} + \frac{w,_r}{r})(2\alpha_o C_o + \frac{4H}{R^2} \alpha_o \beta_o w - \alpha_o \beta_o \int_o^r \frac{w,_x^2}{x} \, dx)$$

$$- (\frac{2H}{R^2} \beta_o^2 w + C_o \beta_o) \int_o^r \frac{w,_x^2}{x} \, dx + \frac{4H}{R^2} \beta_o C_o w \; ;$$

$$\psi,_r \Big|_o^R = - \frac{\beta_o}{2R} \int_o^R r \left(\int_o^r \frac{w,_x^2}{x} \, dx\right) dr + \frac{2H\beta_o}{R^3} \int_o^R rwdr + \frac{C_o R}{2} \tag{B.16}$$

where

$$\alpha_o = e \left(\frac{\lambda_o}{1 + \lambda_o}\right) \mu E^p \; ; \tag{B.17}$$

$$\beta_o = \frac{E^p}{1 + \lambda_o} [(1 + \lambda_o)^2 - \mu^2] \tag{B.18}$$

and

$$C_o = \beta_o \left(\frac{1 + \lambda_o + \mu}{1 + \lambda_o - \mu}\right) \left\{ \frac{1 + \lambda_o}{1 + \lambda_o + \mu} \int_o^R \frac{w,_r^2}{r} \, dr \right.$$

$$\left. - \frac{1}{R^2} \int_o^R r \left(\int_o^r \frac{w,_x^2}{x} \, dx\right) dr + \frac{4H}{R^4} \int_o^R rwdr \right\} . \tag{B.19}$$

Substitution of Equations (B.15) and (B.16) into Equation (B.14) gives the strain energy function in terms of structural and geometric parameters and the normal displacement, w.

$$
\begin{aligned}
U = \frac{\pi}{\beta_o} \int_o^R & \left\{ \alpha_o^2 \left(w_{,rr} + \frac{w_{,r}}{r} \right)^2 + \frac{\beta_o^2}{4} \left(\int_o^r \frac{w_{,x}^2}{x}\, dx \right)^2 \right. \\
& + \left(\frac{2H\beta_o w}{R^2} \right)^2 + C_o^2 + \left(w_{,rr} + \frac{w_{,r}}{r} \right) [2\alpha_o C_o \\
& + \frac{4H}{R^2} \alpha_o \beta_o w - \alpha_o \beta_o \int_o^r \frac{w_{,x}^2}{x}\, dx] \\
& - \left[\frac{2H}{R^2} \beta_o^2 w + C_o \beta_o \right] \int_o^r \frac{w_{,x}^2}{x}\, dx + \frac{4H}{R^2} \beta_o C_o w \right\} r\, dr \qquad (B.20) \\
& - \frac{\pi}{\beta_o} \left(\frac{1 + \lambda_o + \mu}{1 + \lambda_o} \right) \left\{ - \frac{\beta_o}{2R} \int_o^R r \left(\int_o^r \frac{w_{,x}^2}{x}\, dx \right) dr + \frac{2H\beta_o}{R^3} \int_o^R rw\, dr \right. \\
& + \left. \frac{C_o R}{2} \right\}^2 \\
& - \pi \left\{ \frac{(eE^s)^2}{\beta_o} - D(1 + \rho_o + 12\lambda_o \frac{e^2}{h^2}) \right\} \int_o^R \left(w_{,rr} + \frac{w_{,r}}{r} \right)^2 r\, dr
\end{aligned}
$$

APPENDIX C

THE ECCENTRICALLY STIFFENED THIN CIRCULAR PLATE

The thin circular plate of isotropic and elastic material is stiffened eccentrically along the direction of the polar coordinate system in such a way that

i)   the stiffeners are one-sided,

ii)   the eccentricity is the same for all stiffeners and is constant,

iii)   the "smeared" extensional and flexural stiffness is the same for all stiffeners and is constant.

In the derivation of the buckling equations, the von Kármán kinematic relations are used, and the Kirchhoff-Love hypotheses for the combined sheet-stiffener system as used by Baruch and Singer [24] are employed.

The midsurface of the sheet is taken as the reference and the midsurface kinematic relations are:

$$\left.\begin{aligned}
\varepsilon_{rr} &= u,_r \; ; \\
\varepsilon_{\theta\theta} &= \frac{1}{r}(v,_\theta + u) \; ; \\
\varepsilon_{r\theta} &= \frac{1}{2r}(rv,_r + u,_\theta - v) \; ;
\end{aligned}\right\} \quad (C.1)$$

$$\left.\begin{aligned}
\phi_r &= -\, w,_r \; ; \\
\phi_\theta &= -\frac{1}{r} w,_\theta \; ;
\end{aligned}\right\} \quad (C.2)$$

$$\kappa_{rr} = - w,_{rr} \quad ;$$

$$\kappa_{\theta\theta} = - \frac{1}{r} \left(\frac{1}{r} w,_{\theta\theta} + w,_r \right) \quad ;$$

$$\kappa_{r\theta} = - \frac{1}{r} \left(w,_{r\theta} - \frac{1}{r} w,_\theta \right) \quad . \qquad (C.3)$$

Also, the strains at any material point may be expressed in terms of the reference surface strains and changes in curvature and torsion.

$$\varepsilon_r = \varepsilon_{rr} + \eta\kappa_{rr}$$

$$\varepsilon_\theta = \varepsilon_{\theta\theta} + \eta\kappa_{\theta\theta} \qquad (C.4)$$

$$\gamma = \gamma_{r\theta} + 2\eta\kappa_{r\theta}$$

The assumptions that before, and at the instant of buckling, no material point is stressed beyond the proportional limit and the stiffener Poisson effect is negligible are made. One may write for the sheet

$$\sigma_r^p = \frac{E}{1-\mu^2} \left(\varepsilon_r + \mu\varepsilon_\theta \right) \quad ;$$

$$\sigma_\theta^p = \frac{E}{1-\mu^2} \left(\varepsilon_\theta + \mu\varepsilon_r \right) \quad ; \qquad (C.5)$$

$$\tau_{r\theta} = \frac{E}{2(1 + \mu)} \gamma$$

and for the stiffeners

$$\left.\begin{array}{l} \sigma_r^S = E_r \varepsilon_r \ ; \\ \\ \\ \sigma_\theta^S = E_0 \varepsilon_\theta \ . \end{array}\right\} \quad (C.6)$$

It is assumed that the shear is carried entirely by the sheet.

Denoting by N_r, N_θ and $N_{r\theta}$ the stress resultants, and by M_r, M_θ and $M_{r\theta}$ the moment the following may be written for the combined system

$$\left.\begin{array}{l} N_i = \displaystyle\int_{-h/2}^{h/2} \sigma_i^p d\eta + \frac{1}{\ell_i} \int_{\textcircled{A_i}} \sigma_i^S \ dA_i \ ; \\ \\ \\ \\ M_i = \displaystyle\int_{-h/2}^{h/2} \eta \sigma_i^p d\eta + \frac{1}{\ell_i} \int_{\textcircled{A_i}} \sigma_i^S \eta dA_i \end{array}\right\} \quad (C.7)$$

The constitutive relations for the eccentrically stiffened plate are derived and given by

$$\left.\begin{array}{l} N_r = (E^P + E_r^S)\varepsilon_{rr} + \mu E^P \varepsilon_{\theta\theta} + e_r E_r^S \kappa_{rr} \ ; \\ \\ N_\theta = \mu E^P \varepsilon_{rr} + (E^P + E_\theta^S)\varepsilon_{\theta\theta} + e_\theta E_\theta^S \kappa_{\theta\theta} \ ; \\ \\ N_{r\theta} = \dfrac{Eh}{2(1+\mu)} \ \gamma_{r\theta} \ ; \end{array}\right\} \quad (C.8)$$

$$M_r = (D + D_r^S)\kappa_{rr} + \mu D\kappa_{\theta\theta} + e_r^S E_r^S \kappa_{rr} + e_r E_r^S \epsilon_{rr} \; ;$$

$$M_\theta = \mu D\kappa_{rr} + (D + D_\theta^S)\kappa_{\theta\theta} + e_\theta^S E_\theta^S \kappa_{\theta\theta} + e_\theta E_\theta^S \epsilon_{\theta\theta} \; ; \qquad \Bigg\} \quad (C.9)$$

$$M_{r\theta} = D(1 - \mu)\kappa_{r\theta}$$

where

$$E^p = \frac{Eh}{1 - \mu^2} \; ; \qquad E_r^S = \frac{E_r A_r}{\ell_r} \; ; \qquad E_\theta^S = \frac{E_0 A_\theta}{\ell_\theta} \; ;$$

$$E_\theta^S = \frac{E_\theta I_{\theta_{c.g.}}}{\ell_\theta} \; ; \qquad D_r^S = \frac{E_r I_{r_{c.g.}}}{\ell_r} \qquad \Bigg\} \quad (C.10)$$

and A_i and $I_{i_{c.g.}}$ are the cross-sectional area and the second moment of the area about centroidal axes of the stiffeners respectively.

Next, if A_r and $I_{r_{c.g.}}$ are taken to vary linearly, as ℓ_r does, then E_r^S and D_r^S are constant. Furthermore, if $E_r^S = E_\theta^S = E^S$, $D_r^S = D_\theta^S = D^S$ and $e_r = e_\theta = e$ the constitutive relations become

$$N_r = (E^p + E^S)\epsilon_{rr} + \mu E^p \epsilon_{\theta\theta} + eE^S \kappa_{rr} \; ;$$

$$N_\theta = \mu E^p \epsilon_{rr} + (E^p + E^S)\epsilon_{\theta\theta} + eE^S \kappa_{\theta\theta} \; ; \qquad \Bigg\} \quad (C.11)$$

$$N_{r\theta} = \frac{Eh}{2(1 + \mu)} \gamma_{r\theta} \; ;$$

$$M_r = (D + D^s)\kappa_{rr} + \mu D\kappa_{\theta\theta} + e^2 E^s \kappa_{rr} + e E^s \varepsilon_{rr} \; ;$$

$$M_\theta = \mu D\kappa_{rr} + (D + D^s)\kappa_{\theta\theta} + e^2 E^s \kappa_{\theta\theta} + e^2 E^s \varepsilon_{\theta\theta} \; ;$$

$$M_{r\theta} = D(1 - \mu)\kappa_{r\theta}.$$

(C.12)

The equilibrium and compatibility equations for the plate in polar coordinates are given below:

$$N_r + rN_{r,r} + N_{r\theta,\theta} - N_\theta = 0 \; ;$$

$$N_\theta + rN_{r\theta,r} + 2 N_{r\theta} = 0 \; ;$$

$$rM_{r,rr} + 2 M_{r,r} + 2 M_{r\theta,r\theta} - M_{\theta,r} + \frac{1}{r} (M_{\theta,\theta} + 2 M_{r\theta}),_\theta$$

$$+ N_\theta w,_r + rN_r w,_{rr} + 2 N_{r\theta} w,_{r\theta} - \frac{2}{r} N_{r\theta} w,_\theta$$

$$+ \frac{N_\theta}{r} w,_{\theta\theta} = 0 \; ;$$

$$\varepsilon_{\theta\theta,rr} + \frac{1}{r^2} \varepsilon_{rr,\theta\theta} + \frac{2}{r}\varepsilon_{\theta\theta,r} - \frac{1}{r} \varepsilon_{rr,r} - \frac{1}{r} \gamma_{r\theta,r\theta} - \frac{1}{r^2}\gamma_{r\theta,\theta} = 0.$$

(C.13)

If the plate is assumed to deform in a primary state (w=0) up to the point of buckling, then by considering equilibrium states which differ only slightly from the primary state, the basic equations can be linearized by assuming small changes in all quantities involved. Denoting by superscript "1" these small additional changes, and by superscript "o" the membrane state quantities, one may write

$$N = N^o + N^1 \; ;$$

$$N,_\alpha = N^1,_\alpha \quad ;$$

$$M = M^1 \quad ;$$

$$\phi_i = \phi_i^1 \quad ;$$

where $|N^\circ| \gg |N^1|$ and for the circular plate under edge thrust it can be shown that

$$N_r^o = N_\theta^o = -\bar{N} \quad ; \quad N_{r\theta}^o = 0.$$

Linearization of the equilibrium and compatibility equations gives the following

$$\left. \begin{aligned} &N_r^1 + rN_{r,r}^1 + N_{r\theta,\theta}^1 - N_\theta^1 = 0 \quad ; \\[2ex] &N_{\theta,\theta}^1 + rN_{r\theta,r}^1 + 2\,N_{r\theta}^1 = 0 \quad ; \\[2ex] &rM_{r,rr}^1 + 2\,M_{r,r}^1 + 2\,M_{r\theta,r\theta}^1 \quad -M_{\theta,r}^1 + \frac{1}{r}\,(M_{\theta,\theta}^1 + 2\,M_{r\theta}^1) \\[2ex] &\quad - r\,\bar{N}\,(w_{,rr}^1 + \frac{1}{r}\,w_{,r}^1 + \frac{1}{r^2}\,w_{,\theta\theta}^1) = 0 \quad ; \end{aligned} \right\} \quad \text{(C.14)}$$

$$\varepsilon_{\theta\theta,rr}^1 + \frac{1}{r^2}\,\varepsilon_{rr,\theta\theta}^1 + \frac{2}{r}\,\varepsilon_{\theta\theta,r}^1 - \frac{1}{r}\,\varepsilon_{rr,r}^1 - \frac{1}{r}\,\gamma_{r\theta,r\theta}^1 - \frac{1}{r^2}\,\gamma_{r\theta,\theta}^1 = 0.$$

$$\text{(C.15)}$$

The constitutive relations are then written as

$$N_r^1 = (E^P + E^S)\, \varepsilon_{rr}^1 + \mu E^P \varepsilon_{\theta\theta}^1 + eE^S \kappa_{rr}^1 \;;$$

$$N_\theta^1 = \mu E^P \varepsilon_{rr}^1 + (E^P + E^S)\varepsilon_{\theta\theta}^1 + eE^S \kappa_{\theta\theta}^1 \;;$$

$$N_{r\theta}^1 = \frac{E}{2(1 + \mu)} \; \gamma_{r\theta}^1 \;;$$

$$\text{(C.16)}$$

$$M_r^1 = D(\kappa_{rr}^1 + \mu\kappa_{\theta\theta}^1) + eE^S \varepsilon_{rr}^1 + (D^S + e^2 E^S)\kappa_{rr}^1 \;;$$

$$M_\theta^1 = D(\kappa_{\theta\theta}^1 + \mu\kappa_{rr}^1) + eE^S \varepsilon_{\theta\theta}^1 + (D^S + e^2 E^S)\kappa_{\theta\theta}^1 \;;$$

$$M_{r\theta}^1 = D(1 - \mu)\kappa_{r\theta}^1 \;.$$

$$\text{(C.17)}$$

The boundary conditions can be written in the following manner. The clamped support existing at the boundary $r = R$ will be defined by the equations

$$w^1 = 0 \;; \qquad\qquad\qquad\qquad\qquad\qquad\qquad \text{(C.18)}$$

$$w_{,r}^1 = 0 \qquad\qquad\qquad\qquad\qquad\qquad\qquad \text{(C.19)}$$

at $r = R$ and for all θ. The remaining two conditions must be selected from four possible combinations of in-plane constraints on the boundary. The combinations will be designated by a number attached to the code CC

implying the nature of clamped support. Increasing numbers correspond to stronger constraints at r = R. The four sets of conditions are

$$(1) \quad N_r^1 = N_{r\theta}^1 = 0 \; ; \qquad\qquad (C.20)$$

$$(2) \quad u^1 = N_{r\theta}^1 = 0 \; ; \qquad\qquad (C.21)$$

$$(3) \quad v^1 = N_r^1 = 0 \; ; \qquad\qquad (C.22)$$

$$(4) \quad u^1 = v^1 = 0 \; . \qquad\qquad (C.23)$$

Now, introducing the stress function

$$\left. \begin{aligned} N_r^1 &= \frac{1}{r} \, \psi,_{rr} + \frac{1}{r^2} \, \psi,_{\theta\theta} \; ; \\[2ex] N_\theta^1 &= \psi,_{rr} \; ; \\[2ex] N_{r\theta}^1 &= \frac{1}{r^2} \, \psi,_{\theta} - \frac{1}{r} \, \psi,_{r\theta} \end{aligned} \right\} \qquad (C.24)$$

it can be shown that the first two of Equations (C.14) are identically satisfied and through the use of Equations (C.20)–(C.23) and the linearized version of the strain-displacement relations, Equation (C.1), that the third of Equations (C.14) can be written as

$$\frac{\bar{N}}{D} \nabla^2 w^1 - \left[1 + \rho_o + 12 \lambda_o \frac{e^2}{h^2} \right] \nabla^4 w^1 + 2 \left[\rho_o + 12 \lambda_o \frac{e^2}{h^2} \right] L_1 w^1$$

$$- 12 \lambda_o \frac{e^2}{h^2} \frac{\lambda_o}{[(1 + \lambda_o)^2 - \mu^2]} \left[(1 + \lambda_o) \nabla^4 w^1 - 2(1 + \lambda_o + \mu) L_1 w^1 \right] \qquad (C.25)$$

$$+ \frac{\lambda_o e}{D[(1 + \lambda_o)^2 - \mu^2]} \left[\mu \nabla^4 \psi - 2(1 + \lambda_o + \mu) L_1 \psi \right] = 0$$

where ∇^2 is the Laplacian operator, $L_1( ) = \frac{1}{r^2} [( ),_{rr} - \frac{1}{r} ( ),_r$

$+ \frac{1}{r^2} ( )],_{\theta\theta}$ and λ_o, ρ_o are $\frac{E^s}{E^p}$ and $\frac{D^s}{D}$ respectively. Similarly, the compatibility Equation (C.15) can be written

$$(1 + \lambda_o) \nabla^4 \psi + 2 \lambda_o \left(\frac{1 + \lambda_o + \mu}{1 - \mu} \right) L_1 \psi$$

$$(C.26)$$

$$= e \lambda_o E^p \left[\nabla^4 w^1 - 2 \left(\frac{1 + \lambda_o + \mu}{\mu} \right) L_1 w^1 \right].$$

Solution of the Problem for Axisymmetric Buckling

For the circular plate, assuming axisymmetric buckling, Equations (C.25) and (C.26) can be readily solved. Removing all θ dependence and combining into a single equation involving only $\bar{N}$ and w^1 yields

$$\nabla^4 w^1 + \frac{\bar{N}}{D} \left[\frac{1}{1 + \rho_o + 12 \frac{\lambda_o}{1 + \lambda_o} \frac{e^2}{h^2}} \right] \nabla^2 w^1 = 0 \tag{C.27}$$

or, written in another form

$$\nabla^4 w^1 + \rho^2 \nabla^2 w^1 = 0 \ . \tag{C.28}$$

The solution can easily be shown, by requiring finiteness of w^1 at $r = 0$, to be

$$w^1 = A_o [J_o(\rho r) + A_1] \ . \tag{C.29}$$

The stress function ψ can be found by solving the compatibility equation

$$\nabla^4 \psi = e \, \lambda_o \left(\frac{\mu}{1 + \lambda_o} \right) E^P \nabla^4 w^1 \ . \tag{C.30}$$

Using Equation (C.29), Equation (C.30) can be integrated to give

$$\psi = A_o e \mu \left(\frac{\lambda_o}{1 + \lambda_o} \right) E^P J_o(\rho r) + \left(\frac{c_o r^2}{4} + c_2 \right) \ln r + c_4 \frac{r^2}{4} + c_3 \ . \tag{C.31}$$

But, by requiring finiteness of stresses at the center this may be reduced to

$$\psi = e\mu \left(\frac{\lambda_o}{1 + \lambda_o} \right) E^P A_o J_o(\rho r) + c_4 \frac{r^2}{4} + c_3 \ . \tag{C.32}$$

It is now possible to define the characteristic value problem by means of the solutions of the equilibrium and compatibility equations, the boundary conditions, Equations (C.18) and (C.19), and any one of the groups of additional in-plane boundary conditions, Equations (C.20) to (C.23).

Buckling Loads for the Clamped Cases

The buckling equation can be obtained from Equation (C.18) and (C.19) without any dependence on the auxiliary in-plane conditions specified. From the boundary condition $w,_r^1 = 0$ the equation

$$J_o'(\rho R) = 0 \tag{C.33}$$

is obtained thus giving

$$\bar{N} = 14.684 \frac{D}{R^2} \left[1 + \rho_o + 12 \left(\frac{\lambda_o}{1 + \lambda_o} \right) \frac{e^2}{h^2} \right] \tag{C.34}$$

which is identical to that derived by Bryan [28] when unstiffened geometry is used.

LITERATURE CITED

1. Harari, O., Singer, J., and Baruch, M., "General Instability of Cylindrical Shells with Non-uniform Stiffeners," Israel Journal of Technology, Vol. 5, No. 1-2, 1967, pp. 114-128.

2. Cole, R. T., "An Analysis on the General Instability of Eccentrically Stiffened Complete Spheres under Pressure," Ph.D. Thesis, (in process), Georgia Institute of Technology, Atlanta, Georgia.

3. Van der Neut, A., "The General Instability of Stiffened Cylindrical Shells under Axial Compression," National Luchtvaartlaboratorium Report S314, Vol. XIII, Amsterdam, the Netherlands, 1947, pp. 557-584.

4. von Karman, Th. and Tsien, H. S., "The Buckling of Spherical Shells by External Pressure," Journal of the Aeronautical Sciences, Vol. 7, No. 2, December 1939, pp. 43-50.

5. Suhara, J., "Snapping of Shallow Spherical Shells under Static and Dynamic Loadings," Aeroelastic and Structures Research Laboratory, ASRL TR 76-4, MIT, June 1960.

6. Humphreys, J. S. and Bodner, S. R., "Dynamic Buckling of Shallow Shells under Impulsive Loading," Journal of the Engineering Mechanics Division, Proceedings of the American Society of Civil Engineers, Vol. 88, EM 2, April 1962, pp. 17-36.

7. Budiansky, B. and Roth, R. S., "Axisymmetric Dynamic Buckling of Clamped Shallow Spherical Shells," TN D-1510, 1962, NASA, pp. 597-606.

8. Archer, R. R. and Lange, C. G., "Nonlinear Dynamic Behavior of Shallow Spherical Shells," AIAA Journal, Vol. 3, No. 12, December 1965, pp. 2313-2317.

9. Simitses, G. J., "Axisymmetric Dynamic Snap-through Buckling of Shallow Spherical Caps," AIAA Journal, Vol. 5, No. 5, May 1967, pp. 1019-1021.

10. Lock, M. H., Okubo, S., and Whittier, J. S., Experiments on the Snapping of a Shallow Dome under a Step Pressure Load," AIAA Journal, Vol. 6, No. 7, July 1968, pp. 1320-1326.

11. Stephens, W. B. and Fulton, R. E., "Axisymmetric Static and Dynamic Buckling of Spherical Caps due to Centrally Distributed Pressures,"

Literature Cited (Cont'd.)

AIAA Paper 69-89 (1969).

12. Stricklin, J. A. and Martinez, J. E., "Dynamic Buckling of Clamped Spherical Caps under Step Pressure Loadings," AIAA Journal, Vol. 7, No. 6, June 1969, pp. 1212-1213.

13. Huang, N. C., "Axisymmetric Dynamic Snap-through of Elastic Clamped Shallow Spherical Shells," AIAA Journal, Vol. 7, No. 2, February 1969, pp. 215-220.

14. Bushnell, D., "Nonlinear Axisymmetric Behavior of Shells of Revolution," AIAA Journal, Vol. 5, No. 3, March 1967, pp. 432-439.

15. Bushnell, D., "Symmetric and Nonsymmetric Buckling of Finitely Deformed Eccentrically Stiffened Shells of Revolution," AIAA Journal, Vol. 5, No. 8, August 1967, pp. 1455-1462.

16. Ebner, H., "Angenaherte Bestimmung der Tragfahigkeit radial versteifter Kugelschalen unter Druckbelastung," Proceedings of the Symposium on the Theory of Thin Elastic Shells, edited by W. T. Koiter, North-Holland Publishing Co., Amsterdam, the Netherlands, 1960, pp. 95-121.

17. Crawford, R. F. and Schwartz, D. B., "General Instability and Optimum Design of Grid-stiffened Spherical Domes," AIAA Journal, Vol. 3, No. 3, March 1965, pp. 511-515.

18. Crawford, R. F., "Effects of Asymmetric Stiffening on Buckling of Shells," AIAA Paper 65-371 (1965).

19. Budiansky, B., "Buckling of Clamped Shallow Spherical Shells," Proceedings of the Symposium on the Theory of Thin Elastic Shells, edited by W. T. Koiter, North-Holland Publishing Co., Amsterdam, the Netherlands, 1960, pp. 64-94.

20. Reissner, E., "On Axisymmetric Vibrations of Shallow Spherical Shells," Quarterly of Applied Mathematics, Vol. 13, 1955, pp. 279-290.

21. Reissner, E., "On Transverse Vibrations of Thin Shallow Elastic Shells," Quarterly of Applied Mathematics, Vol. 13, 1955, pp. 169-176.

22. Humphreys, J. S., "On the Adequacy of Energy Criteria for Dynamic Buckling of Arches," AIAA Journal, Vol. 4, No. 5, May 1966, pp. 921-923.

23. Sanders, J. L., Jr., "Nonlinear Theories for Thin Shells," *Quarterly of Applied Mathematics*, Vol. 21, 1963, pp. 21-36.

24. Baruch, M. and Singer, J., "Effect of Eccentricity of Stiffeners on the General Instability of Stiffened Cylindrical Shells under Hydrostatic Pressure," *Journal of Mechanical Engineering Sciences*, Vol. 5, No. 1, 1963, pp. 23-27.

25. Thurston, G. A., "A Numerical Solution of the Nonlinear Equations for Axisymmetric Bending of Shallow Spherical Shells," *Journal of Applied Mechanics, Transactions of the A.S.M.E.*, Vol. 28, 1961, pp. 557-562.

26. Archer, R. R., "On the Numerical Solution of the Nonlinear Equations for Shells of Revolution," *Journal of Mathematics and Physics*, Vol. 40, No. 3, 1962, pp. 165-179.

27. Weinitschke, H. J., "On the Stability Problem for Shallow Spherical Shells," *Journal of Mathematics and Physics*, Vol. 38, No. 3, 1960, pp. 209-231.

28. Bryan, G. H., "Buckling of Plates," *Proceedings of the London Mathematical Society*, Vol. 22, 1891, p. 54.

VITA

Charles Mcsween Blackmon, son of Mr. and Mrs. Charlie H. Blackmon, was born on January 16, 1940 in Montgomery, Alabama. After moving to Marietta, Georgia he attended the public schools of that city and was graduated from Marietta High School in 1958.

In September, 1958, Mr. Blackmon entered the Georgia Institute of Technology and received the degree of Bachelor of Aeronautical Engineering in June, 1962. Continuing his education there, he received the degree of Master of Science in Aerospace Engineering in June, 1963.

He was employed as an engineer by the Fort Worth Division of General Dynamics Corporation from June, 1963 until September, 1966. He married the former Margaret VanDeman in March, 1964. He returned in September, 1966 to the Georgia Institute of Technology and received a NASA Traineeship to study under the doctoral program.

He is a member of the Sigma Gamma Tau and Tau Beta Pi Honor Societies.